NON-PARAMETRIC NEURO-ADAPTIVE CONTROL SUBJECT TO TASK SPECIFICATIONS

Christos K. Verginis
Oden Institute for Computational Engineering and Sciences
University of Texas at Austin
Austin, TX78705, USA
cverginis@utexas.edu

Zhe Xu
School for Engineering of Matter,
Transport, and Energy
Arizona State University
Tempe, AZ85281, USA
xzhe1@asu.edu

Ufuk Topcu
Oden Institute for Computational Engineering and Sciences
University of Texas at Austin
Austin, TX78705, USA
utopcu@utexas.edu

ABSTRACT

We develop a learning-based algorithm for the control of autonomous systems governed by unknown, nonlinear dynamics to satisfy user-specified spatio-temporal tasks expressed as signal temporal logic specifications. Most existing algorithms either assume certain parametric forms for the unknown dynamic terms or resort to unnecessarily large control inputs in order to provide theoretical guarantees. The proposed algorithm addresses these drawbacks by integrating neural-network-based learning with adaptive control. More specifically, the algorithm learns a controller, represented as a neural network, using training data that correspond to a collection of system parameters and tasks. These parameters and tasks are derived by varying the nominal parameters and the spatio-temporal constraints of the user-specified task, respectively. It then incorporates this neural network into an online closed-form adaptive control policy in such a way that the resulting behavior satisfies the user-defined task. The proposed algorithm does not use any a priori information on the unknown dynamic terms or any approximation schemes. We provide formal theoretical guarantees on the satisfaction of the task. Numerical experiments on a robotic manipulator and a unicycle robot demonstrate that the proposed algorithm guarantees the satisfaction of 50 user-defined tasks, and outperforms control policies that do not employ online adaptation or the neural-network controller. Finally, we show that the proposed algorithm achieves greater performance than standard reinforcement-learning algorithms in the pendulum benchmarking environment.

1 INTRODUCTION

Learning and control of autonomous systems with uncertain dynamics is a critical and challenging topic that has been widely studied during the last decades. One can identify plenty of motivating reasons, ranging from uncertain geometrical or dynamical parameters and unknown exogenous disturbances to abrupt faults that significantly modify the dynamics. There has been, therefore, an increasing need for developing control algorithms that do not rely on the underlying system dynamics. At the same time, such algorithms can be easily implemented on different, heterogeneous systems, since one does not need to be occupied with the tedious computation of the dynamic terms.

There has been a large variety of works that tackle the problem of control of autonomous systems with uncertain dynamics, exhibiting, however, certain limitations. The existing algorithms are based on adaptive and learning-based approaches or the so-called funnel control (Krstic et al. (1995); Vamvoudakis & Lewis (2010); Berger et al. (2018); Bechlioulis & Rovithakis (2014); Joshi et al.

(2020); Capotondi et al. (2020); Bertsekas & Tsitsiklis (1996); Sutton & Barto (2018)). Nevertheless, adaptive control methodologies are restricted to system dynamics that can be linearly parameterized with respect to certain unknown parameters (e.g., masses, moments of inertia), assuming the system structure perfectly known; funnel controllers employ reciprocal terms that drive the control input to infinity when the tracking error approaches a pre-specified funnel function, creating thus unnecessarily large control inputs that might damage the system actuators. Data-based learning approaches either consider some system characteristic known (e.g., a nominal model, Lipschitz constants, or global bounds), or use neural networks to learn a tracking controller or the system dynamics; the correctness of such methods, however, relies on strong assumptions on the parametric approximation by the neural network and knowledge of the underlying radial basis functions. Finally, standard reinforcement-learning techniques (Bertsekas & Tsitsiklis (1996); Sutton & Barto (2018)) usually assume certain state and/or time discretizations of the system and rely on exhaustive search of the state space, which might lead to undesirable transient properties (e.g., collision with obstacles while learning).

1.1 Contributions and Significance

This paper addresses the control of systems with continuous, *unknown* nonlinear dynamics subject to task specifications expressed as signal interval temporal logic (SITL) constraints (Lindemann & Dimarogonas (2020)). Our main contribution lies in the development of a learning-based control algorithm that guarantees the accomplishment of a given task using only mild assumptions on the system dynamics. The algorithm draws a novel connection between adaptive control and learning with neural network representations, and consists of the following steps. Firstly, it trains a neural network that aims to learn a controller that accomplishes a given task from data obtained off-line. Secondly, it calculates an open-loop trajectory that yields the execution of the task if followed by the system, while neglecting the dynamics. Finally, we develop an online adaptive feedback control policy that uses the trained network to guarantee convergence to the open-loop trajectory and hence satisfaction of the task. Essentially, our approach builds on a combination of off-line trained controllers and on-line adaptations, which was recently shown to significantly enhance performance with respect to single use of the off-line part (Bertsekas (2021)). The proposed approach is particularly suitable for cases when engineering systems undergo purposeful modifications (e.g., the substitution of a motor/link in a robotic arm or exposure to new working environments) which might change their dynamics or operating conditions. In such cases, the goal is not to re-design new model-based controllers for the modified systems, but rather exploit the already designed ones and guarantee correctness via intelligent online adaptation policies.

The major significance of our contribution is twofold. Firstly, we guarantee the theoretical correctness of the proposed algorithm by considering only mild conditions on the neural network, removing the long-standing assumptions on parametric approximations and boundedness of the estimation error. Secondly, we demonstrate via the experimental results the generality of the algorithm with respect to different tasks and system parameters. That is, the training data that we generate for the training of the neural network in the first step correspond to tasks that are different, in terms of spatiotemporal specifications, from the given one to be executed[1]. Additionally, we employ systems with different dynamic parameters to generate these data. We evaluate the proposed algorithm in numerous scenarios comprising different variations of the given task and different system dynamic parameters, which do not necessarily match the training data. We show that the algorithm, owing to its adaptation properties, is able to guarantee the satisfaction of the respective tasks in all the aforementioned scenarios by using the same neural network.

1.2 Related work

A large variety of previous works considers neuro-adaptive control with stability guarantees, focusing on the optimal control problem (Vamvoudakis & Lewis (2010); Yang et al. (2020); Cheng et al. (2007); Fan et al. (2018); Kiumarsi et al. (2017); Zhao & Gan (2020); Vrabie & Lewis (2009); Sun & Vamvoudakis (2020); Kamalapurkar et al. (2015); Huang et al. (2018b); Mo et al. (2019); Joshi et al. (2020)). Nevertheless, the related works draw motivation from the neural network density property (see, e.g., (Cybenko (1989)))[2] and assume sufficiently small approximation errors and linear

[1] The task difference is illustrated in Section 4.

[2] A sufficiently large neural network can approximate a continuous function arbitrarily well in a compact set.

parameterizations of the unknown terms (dynamics, optimal controllers, or value functions), which is also the case with traditional adaptive control methodologies (Krstic et al. (1995); Hong et al. (2009); Chen (2019); Huang et al. (2018a)). This paper relaxes the aforementioned assumptions and proposes a *non-parametric* neuro-adaptive controller, whose stability guarantees rely on a mild boundedness condition of the closed-loop system state that is driven by the learned controller. The proposed approach exhibits similarities with (Liu et al. (1994)), which employs off-line-trained neural networks with online feedback control, but fails to provide convergence guarantees.

Other learning-based related works include modeling with Gaussian processes (Capotondi et al. (2020); Leahy et al. (2019); Jain et al. (2018); Berkenkamp & Schoellig (2015)), or use neural networks (Ma et al. (2020); Shah et al. (2018); Yan & Julius (2021); Liu et al. (2021); Hahn et al. (2020); Cai et al. (2021); Wang et al. (2020); Camacho & McIlraith (2019); Hahn et al. (2020); Riegel et al. (2020); Hu et al. (2020); Ivanov et al. (2019)) to accomplish reachability, verification or temporal logic specifications. Nevertheless, the aforementioned works either use partial information on the underlying system dynamics, or do not consider them at all. In addition, works based on Gaussian processes usually propagate the dynamic uncertainties, possibly leading to conservative results. Similarly, data-driven model-predictive control techniques (Nubert et al. (2020); Maddalena et al. (2020)) use data to over-approximate additive disturbances or are restricted to linear systems.

Control of unknown nonlinear continuous-time systems has been also tackled in the literature by using funnel control, without necessarily using off-line data or dynamic approximations (Berger et al. (2018); Bechlioulis & Rovithakis (2014); Lindemann et al. (2017); Verginis & Dimarogonas (2018); Verginis et al. (2021)). Nevertheless, funnel controllers usually depend on reciprocal time-varying barrier functions that drive the control input to infinity when the error approaches a pre-specified funnel, creating thus unnecessarily large control inputs that might damage the system actuators.

2 Preliminaries and Problem Formulation

2.1 Signal interval temporal logics

Let $y : \mathbb{R}_{\geq 0} \to \mathbb{R}^n$ be a continuous-time signal. Signal interval temporal logic (SITL) consists of predicates μ that are obtained after evaluation of a continuously differentiable predicate function $h : \mathbb{R}^n \to \mathbb{R}$ (Lindemann & Dimarogonas (2020)). For $\zeta \in \mathbb{R}^n$, let $\mu \coloneqq \top$ if $h(\zeta) \geq 0$ and $\mu \coloneqq \bot$ if $h(\zeta) < 0$. The SITL syntax is given by

$$\varphi \coloneqq \top \mid \mu \mid \neg\varphi \mid \varphi_1 \wedge \varphi_2 \mid \varphi_1 U_{[a,b]} \varphi_2,$$

where φ_1 and φ_2 are SITL formulas, $[a, b] \subset \mathbb{R}_{\geq 0}$, with $b > a$ is a time interval, and $U_{[a,b]}$ encodes the until operator. Define the eventually and always operators as $F_{[a,b]}\varphi \coloneqq \top U_{[a,b]}\varphi$ and $G_{[a,b]}\varphi \coloneqq \neg F_{[a,b]}\neg\varphi$. The satisfaction relation $(y, t) \models \varphi$ denotes that the signal $y : \mathbb{R}_{\geq 0} \to \mathbb{R}^n$ satisfies φ at time t. The SITL semantics are recursively given by $(y, t) \models \mu$ if and only if $h(y(t)) \geq 0$, $(y, t) \models \neg\varphi$ if and only if $\neg((y, t) \models \varphi)$, $(y, t) \models \varphi_2 \wedge \varphi_2$ if and only if $(x, t) \models \varphi_1$ and $(y, t) \models \varphi_2$, and $(y, t) \models \varphi_1 U_{[a,b]} \varphi_2$ if and only if there exists a $t_1 \in [t + a, t + b]$ such that $(y, t_1) \models \varphi_2$ and $(y, t_2) \models \varphi_1$, for all $t_2 \in [t, t_1]$. A formula φ is satisfiable if there exists a $y : \mathbb{R}_{\geq 0} \to \mathbb{R}^n$ such that $(y, 0) \models \varphi$.

2.2 Problem Statement

Consider a continuous-time dynamical system governed by the 2nd-order continuous-time dynamics

$$\ddot{x} = f(\bar{x}, t) + g(\bar{x}, t)u(\bar{x}, t), \tag{1}$$

where $\bar{x} \coloneqq [x^\top, \dot{x}^\top]^\top \in \mathbb{R}^{2n}$, $n \in \mathbb{N}$, is the system state, assumed available for measurement,and $u : \mathbb{R}^{2n} \times [0, \infty) \to \mathbb{R}^n$ is the time-varying feedback-control input. The terms $f(\cdot)$ and $g(\cdot)$ are nonlinear vector fields that are locally Lipschitz in $\bar{x}$ over $\mathbb{R}^{2n}$ for each fixed $t \geq 0$, and uniformly bounded in t over $[0, \infty)$ for each fixed $\bar{x} \in \mathbb{R}^{2n}$. The dynamics (1) comprise a large class of nonlinear dynamical systems (Zhong & Leonard (2020); Yu et al. (1996); Doya (1997)) that capture contemporary engineering problems in mechanical, electromechanical and power electronics applications, such as rigid/flexible robots, induction motors and DC-to-DC converters, to name a few. The continuity in time and state provides a direct link to the actual underlying system, and we further do not require any time or state discretizations.

We consider that $f(\cdot)$ and $g(\cdot)$ are completely unknown; we do not assume any knowledge of the structure, Lipschitz constants, or bounds, and we do not use any scheme to approximate them. Nevertheless, we do assume that $g(\bar{x}, t)$ is positive definite:

Assumption 1. *The matrix $g(\bar{x}, t)$ is positive definite, for all $(\bar{x}, t) \in \mathbb{R}^{2n} \times [0, \infty)$.*

Such assumption is a sufficiently controllability condition for (1); intuitively, it states that the multiplier of u (the input matrix) does not change the direction imposed to the system by the underlying control algorithm. Systems not covered by (1) or Assumption 1 consist of underactuated or non-holonomic systems, such as unicycle robots or underactuated aerial vehicles. Nevertheless, we extend our results for a non-holonomic unicycle vehicle in Section 3.3. Moreover, the 2nd-order model (1) can be easily extended to account for higher-order integrator systems (Slotine et al. (1991)).

Consider now a time-constrained task expressed as an SITL formula φ over x. The objective of this paper is to construct a time-varying feedback-control algorithm $u(\bar{x}, t)$ such that the output of the closed-loop system (1) satisfies φ, i.e., $(x(t), t) \models \varphi$.

3 Main Results

This section describes the proposed algorithm, which consists of three steps. Firstly, it learns a controller, represented as a neural network, using training data that correspond to a collection of different tasks and system parameters. Secondly, it uses formal methods tools to compute an *open-loop* trajectory that satisfies the given task. Finally, we design an adaptive, time-varying feedback controller that uses the neural-network approximation and guarantees tracking of the open-loop trajectory, consequently achieving satisfaction of the task.

3.1 Neural-network learning

We assume the existence of offline data from a finite set of T system trajectories that satisfy a collection of SITL tasks, including the one modeled by φ, and possibly produced by systems with different dynamic parameters. The data from each trajectory $i \in \{1, \dots, T\}$ comprise a finite set of triplets $\{\bar{x}_s(t), t, u_s(t)\}_{t \in \mathcal{T}_i}$, where $\mathcal{T}_i$ is a finite set of time instants, $\bar{x}_s(t) \in \mathbb{R}^{2n}$ are system states, and $u_s(t) \in \mathbb{R}^n$ are the respective control inputs, compliant with the dynamics (1). We use the data to train a neural network in order to approximate the respective controller $u(\bar{x}, t)$. More specifically, we use the pairs $(\bar{x}_s(t), t)_{t \in \mathcal{T}_i}$ as input to a neural network, and $u_s(t)_{t \in \mathcal{T}_i}$ as the respective output targets, for all trajectories $i \in \{1, \dots, T\}$. For given $\bar{x} \in \mathbb{R}^{2n}, t \in \mathbb{R}_{\geq 0}$, we denote by $u_{\text{nn}}(\bar{x}, t)$ the output of the neural network. Note that the controller $u(\bar{x}, t)$, which the neural network aims to approximate, is not associated to the specific task modeled by φ and mentioned in Section 2.2, but a collection of SITL tasks. Therefore, we do not expect the neural network to learn how to accomplish this specific task φ, but rather to be able to adapt to the entire collection of tasks. This is an important attribute of the proposed scheme, since it can generalize over the SITL tasks; that is, the specific task φ to be accomplished can be any task of the aforementioned collection. The proposed algorithm, consisting of the trained neural network and the online feedback-control policy - illustrated in the next sections - is still able to guarantee its satisfaction.

3.2 Open-loop trajectory

The next step is the computation of an open-loop trajectory $p_{\text{d}} : \mathbb{R}_{\geq 0} \to \mathbb{R}^n$ that satisfies φ, i.e., $(p_{\text{d}}(t), t) \models \varphi$. For this computation, we use the recent work (Lindemann & Dimarogonas (2020)), which proposes an efficient planning algorithm using automata to construct a set of bounded trajectories that satisfy an SITL formula. In order to accommodate the temporal aspect of an SITL formula, such a trajectory can be represented as a finite prefix followed by the infinite repetition of a finite suffix, i.e., $p_{\text{d}}(t) = p_{\text{d}}(0 : t_{f_1}) \Big| [p_{\text{d}}(t_{f_1} : t_{f_2})]^{\omega}$. Here, $p_{\text{d}}(0 : t_{f_1})$ and $p_{\text{d}}(t_{f_1} : t_{f_2})$ denote the trajectories $p_{\text{d}}(t)$ from 0 to t_{f_1} and from t_{f_1} to t_{f_2} respectively, for some time instants $t_{f_1} > 0$, $t_{f_2} > t_{f_1}$. The operator $\cdot|\cdot$ denotes trajectory concatenation and the superscript ω denotes infinite repetition. Note that the training data of Section 3.1 are assumed to follow this prefix-suffix form; each trajectory is assumed to consist of a finite prefix followed by some repetitions of a finite suffix, i.e., $\max\{\mathcal{T}_i\} > \kappa t_{f_2}$ for some integer $\kappa > 2$ for all trajectories $i \in \{1, \dots, T\}$. The procedure of computing $p_{\mathrm{d}}(t)$ does *not* take into account the dynamics (1); unlike the training data used in Section 3.1, $p_{\mathrm{d}}(t)$ is a geometric trajectory in $\mathbb{R}^n$ that satisfies the given task. More details regarding the procedure are out of scope of this paper and can be found in (Lindemann & Dimarogonas (2020)).

3.3 Feedback control design

As mentioned in Section 3.1, we do not expect the neural-network controller to accomplish the given task, since the system (1) is trained on potentially different tasks and different system parameters, and (2) the neural network provides only an *approximation* of a stabilizing controller; potential deviations in certain regions of the state space might lead to instability. Moreover, the neural-network controller has no error feedback with respect to the open-loop trajectory p_{d}; such feedback is substantial in the stability of control systems with dynamic uncertainties. Therefore, this section is devoted to the design of a feedback-control policy to track the trajectory $p_{\mathrm{d}}(t)$ by using the output of the trained neural network (see Fig. 1a). The goal is to drive the error $e := x - p_{\mathrm{d}}$ to zero. We first impose an assumption on the closed-loop system trajectory that is driven by the neural network's output.

Assumption 2. *The output $u_{\mathrm{nn}}(\bar{x}, t)$ of the trained neural network satisfies*

$$\|f(\bar{x}, t) + g(\bar{x}, t)u_{\mathrm{nn}}(\bar{x}, t)\| \leq d\|\bar{x}\| + B \tag{2}$$

for positive constants d, B, for all $\bar{x} \in \mathbb{R}^{2n}$, $t \geq 0$.

Intuitively, Assumption 2 states that the neural-network controller $u_{\mathrm{nn}}(\bar{x}, t)$ is able to maintain the *boundedness* of the system state by the constants d, B, which are considered to be *unknown*. The assumption is motivated by the property of neural networks to approximate a continuous function arbitrarily well in a compact domain for a large enough number of neurons and layers (Cybenko (1989))[3]. Loosely speaking, since the collection of SITL tasks, which the neural network is trained with, correspond to bounded trajectories, the system states are expected to remain bounded. Since $f(\bar{x}, t)$, and $g(\bar{x}, t)$ are continuous in $\bar{x}$ and bounded in t, they are also expected to be bounded as per (2). Contrary to the related works (e.g., (Vamvoudakis & Lewis (2010); Yang et al. (2020); Cheng et al. (2007); Fan et al. (2018))), however, we do not adopt approximation schemes for the system dynamics and we do not impose restrictions on the size of d, B. Moreover, Assumption 2 does not imply that the neural network controller $u_{\mathrm{nn}}(\bar{x}, t)$ guarantees tracking of the open-loop trajectory p_{d}. Instead, it is merely a growth condition. Additionally, note that inequality 2 does not depend specifically on any of the SITL tasks that the neural network is trained with. We exploit this property in the control design and achieve task generalization; that is, the open-loop trajectory p_{d} to be tracked (corresponding to the task φ) can be any of the tasks that the neural network is trained with.

We now define the feedback-control policy. Consider the adaptation variables $\hat{\ell}_1$, $\hat{\ell}_2$, corresponding to upper bounds of d, B in (2), with $\hat{\ell}_1(0) > 0$, $\hat{\ell}_2(0) > 0$. We design first a reference signal for $\dot{x}$ as

$$v_{\mathrm{d}} := \dot{p}_{\mathrm{d}} - k_1 e, \tag{3}$$

that would stabilize the subsystem $\|e\|^2$, where k_1 is a positive control gain constant. Following the back-stepping methodology (Krstic et al. (1995)), we define next the respective error $e_v := \dot{x} - v_{\mathrm{d}}$ and design the neural-network-based adaptive control law as

$$u(\bar{x}, \hat{\ell}_1, \hat{\ell}_2, t) = u_{\mathrm{nn}}(\bar{x}, t) - k_2 e_v - \hat{\ell}_1 e_v - \hat{\ell}_2 \hat{e}_v \tag{4a}$$

$$\dot{\hat{\ell}}_1 = k_{\ell_1}\|e_v\|^2, \;\; \dot{\hat{\ell}}_2 = k_{\ell_2}\|e_v\| \tag{4b}$$

where $k_2, k_{\ell_1}, k_{\ell_2}$ are positive constants, and $\hat{e}_v = \frac{e_v}{\|e_v\|}$ if $e_v \neq 0$, and $\hat{e}_v = 0$ if $e_v = 0$. The control design is inspired by adaptive control methodologies (Krstic et al. (1995)), where the time-varying gains $\hat{\ell}_1(t)$, $\hat{\ell}_2(t)$, adapt to the unknown dynamics and counteract the effect of d and B in (2) in order to ensure closed-loop stability. Note that the policy (3), (4) does not use any information on the system dynamics $f(\cdot)$, $g(\cdot)$ or the constants B, d. The tracking of p_{d} is guaranteed by the following theorem, whose proof is given in Appendix A.

Theorem 1. *Let a system evolve according to (1) and let an open-loop trajectory $p_{\mathrm{d}}(t)$ that satisfies a given SITL task modeled by φ. Under Assumption 2, the control algorithm (4) guarantees $\lim_{t\to\infty}(e(t), e_v(t)) = 0$, as well as the boundedness of all closed-loop signals.*

[3] For simplicity, we consider that (2) holds globally, but it can be extended to hold in a compact set.

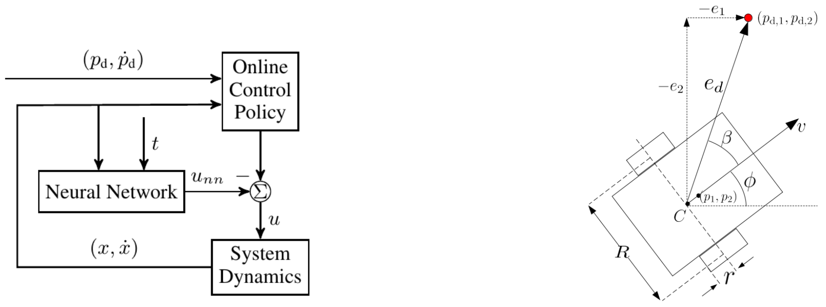

(a) (b)

Figure 1: (a): Block diagram of the proposed algorithm. (b): A unicycle vehicle.

Note that, contrary to works in the related literature (e.g., (Verginis & Dimarogonas (2020); Bechlioulis & Rovithakis (2014))), we do not impose reciprocal terms in the control input that grow unbounded in order to guarantee closed-loop stability. The resulting controller is essentially a simple linear feedback on $(e(t), e_v(t))$ with time-varying adaptive control gains, accompanied by the neural network output that ensures the growth condition (2). The positive gains k_1, k_2, k_{ℓ_1}, k_{ℓ_2} do not affect the stability results of Theorem 1, but might affect the evolution of the closed-loop system; e.g., larger gains lead to faster convergence but possibly larger control inputs.

Extension to non-holonomic unicycle dynamics

As mentioned in Section 1, the dynamics 1 do not represent all kinds of systems, with one particular example being when non-holonomic constraints are present. In such cases, the control law design (4) and Theorem 1 no longer hold. In this section, we extend the control policy to account for unicycle vehicles subject to first-order non-holonomic constraints. More specifically, we consider the dynamics

$$\dot{p}_1 = v\cos\phi, \quad \dot{p}_2 = v\sin\phi, \quad \dot{\phi} = \omega \tag{5a}$$

$$M\ddot{\theta} = u + f_\theta(\bar{x}, t) \tag{5b}$$

where $x = [p_1, p_2, \phi]^\top \in \mathbb{R}^3$ are the unicycle's position and orientation, (v, ω) are its linear and angular velocity (see Fig. 1b), $\theta := [\theta_R, \theta_L]^\top \in \mathbb{R}^2$ are its wheel's angular positions, and $u = [u_R, u_L]^\top \in \mathbb{R}^2$ are the wheel's torques, representing the control input. The unicycle vehicle is subject to the non-holonomic constraint $\dot{p}_1 \sin\phi - \dot{p}_2\cos\phi = 0$, which implies that the vehicle cannot move laterally. Additionally, $M \in \mathbb{R}^{2\times 2}$ is the vehicle's inertia matrix, which is symmetric and positive definite, and $f_\theta(\cdot)$ is a function representing friction and external disturbances. The velocities satisfy the relations $v = \frac{r}{2}(\dot{\theta}_R + \dot{\theta}_L)$, $\omega = \frac{r}{2R}(\dot{\theta}_R - \dot{\theta}_L))$, where r and R are the wheels' radius and axle length, respectively. The terms r, R, M, and $f_\theta(\cdot)$ are considered to be *completely unknown*. As before, the goal is for the vehicle's position $p := [p_1, p_2]^\top$ to track the desired trajectory $p_\mathrm{d} = [p_{\mathrm{d},1}, p_{\mathrm{d},2}]^\top \in \mathbb{R}^2$, which is output from the procedure described in Sec. 3.2. Towards that end, we define the error variables $e_1 := p_1 - p_{\mathrm{d},1}$, $e_2 := p_2 - p_{\mathrm{d},2}$, $e_d := \|p - p_\mathrm{d}\|$, as well as the angle β measured from the the longitudinal axis of the vehicle, i.e., the unicycle's direction vector $[\cos\phi, \sin\phi]$, to the error vector $-[e_1, e_2]$ (see Fig. 1b). The angle β can be derived by using the cross product between the aforementioned vectors, i.e., $e_d\sin(\beta) = [\cos\phi, \sin\phi] \times [-e_1, -e_2] = e_1\sin\phi - e_2\cos\phi$. The purpose of the control design, illustrated next, is to drive e_d and β to zero. By differentiating the latter and using (5) as well as the relations $e_1 = -e_d\cos(\phi + \beta)$, $e_2 = -e_d\sin(\phi + \beta)$ (see Fig. 1b), we derive

$$\dot{e}_d = -v\cos\beta + \dot{p}_{\mathrm{d},1}\cos(\phi + \beta) + \dot{p}_{\mathrm{d},2}\sin(\phi + \beta) \tag{6a}$$

$$\dot{\beta} = -\omega + \frac{\sin\beta}{e_d}v - \frac{\dot{p}_{\mathrm{d},1}}{e_d}\sin(\phi + \beta) + \frac{\dot{p}_{\mathrm{d},2}}{e_d}\cos(\phi + \beta) \tag{6b}$$

In view of (6), we set reference signals for the vehicle's velocity as

$$v_{\text{d}} := \frac{1}{\cos(\beta)}\left(\dot{p}_{\text{d},1}\cos(\beta+\phi) + \dot{p}_{\text{d},2}\sin(\beta+\phi) + k_d e_d\right) \tag{7a}$$

$$\omega_{\text{d}} := -\frac{\sin(\phi)\dot{p}_{\text{d},1}}{\cos(\beta)e_d} + \frac{\cos(\phi)\dot{p}_{\text{d},2}}{\cos(\beta)e_d} + k_d\tan\beta + k_\beta\beta \tag{7b}$$

where k_d, k_β are positive gains, aiming to create exponentially stable subsystems via the terms $k_d e_d$ and $k_\beta\beta$. We define next the respective velocity errors $e_v := v - v_{\text{d}}$, $e_\omega := \omega - \omega_{\text{d}}$ and design the adaptive and neural-network-based control input as $u(\bar{x}, \hat{d}, t) := [\frac{u_S+u_D}{2}, \frac{u_S-u_D}{2}]^\top + u_{\text{nn}}(\bar{x}, t)$, with

$$u_S := \hat{\ell}_v\dot{v}_{\text{d}} - (k_v + \hat{\ell}_1)e_v - \hat{\ell}_2\hat{e}_v + e_d\cos\beta - \beta\frac{\sin\beta}{e_d} \tag{8a}$$

$$u_D := \hat{\ell}_\omega\dot{\omega}_{\text{d}} - (k_\omega + \hat{\ell}_1)e_\omega - \hat{\ell}_2\hat{e}_\omega + \beta \tag{8b}$$

$$\dot{\hat{\ell}}_v := -k_v e_v \dot{v}_{\text{d}}, \qquad \dot{\hat{\ell}}_\omega := -k_\omega e_\omega \dot{\omega}_{\text{d}} \tag{8c}$$

$$\dot{\hat{\ell}}_1 := k_1(e_v^2 + e_\omega^2) \qquad \dot{\hat{\ell}}_2 := k_2(|e_v| + |e_\omega|) \tag{8d}$$

where $\hat{\ell}_v$, $\hat{\ell}_\omega$, $\hat{\ell}_i$ are adaptation variables (similar to (4)), with $\hat{\ell}_v(0) > 0$, $\hat{\ell}_\omega(0) > 0$ and k_v, k_ω, k_i, are positive gains, $i \in \{1, 2\}$; $\hat{e}_a$, with $a \in \{v, \omega\}$, is defined as $\hat{e}_a = \frac{e_a}{|e_a|}$ if $e_a \neq 0$ and $\hat{e}_a = 0$ otherwise. We now re-state Assumption 2 to apply for the unicycle analysis as follows.

Assumption 3. *The output $u_{\text{nn}}(\bar{x}, t)$ of the trained neural network satisfies $\|u_{\text{nn}}(\bar{x}, t) + f_\theta(\bar{x}, t)\| \leq d\|\bar{x}\| + B$, for positive, unknown constants d, B.*

Similar to assumption 2, assumption 3 is merely a growth-boundedness condition by the unknown constants d and B. The stability of the proposed scheme is provided in the next corollary, whose proof is found in Appendix A.

Corollary 1. *Let the unicycle system (5) and let an open-loop trajectory $\text{p}_{\text{d}}(t)$ that satisfies a given SITL task modeled by φ. Assume that $\beta(t) \in (-\bar{\beta}, \bar{\beta})$, $|\dot{p}_{\text{d},1}\sin\phi - \dot{p}_{\text{d},2}\cos\phi| < e_d\alpha_1$, $\sin\beta < e_d\alpha_2$ for positive constants $\bar{\beta} < \frac{\pi}{2}$, α_1, α_2 and all $t \geq 0$. Under Assumption 3, the control policy (8) guarantees $\lim_{t\to\infty}(e_d(t), \beta(t), e_v(t), e_\omega(t)) = 0$, and the boundedness of all closed-loop signals.*

The assumptions $|\dot{p}_{\text{d},1}\sin\phi - \dot{p}_{\text{d},2}\cos\phi| < e_d\alpha_1$, $\sin\beta < e_d\alpha_2$ are imposed to avoid the singularity of $e_d = 0$; note that β and ω_{d} are not defined in that case. Intuitively, they imply that e_d will not be driven to zero faster than β or $\dot{p}_{\text{d},1}\sin\phi - \dot{p}_{\text{d},2}\cos\phi$; the latter becomes zero when the vehicle's velocity vector v aligns with the desired one $\dot{p}_{\text{d}}$. In the experiments, we tune the control gains according to $k_\beta \sim 10k_d$ in order to satisfy these assumptions.

4 Numerical Experiments

This section is devoted to a series of numerical experiments. More details can be found in Appendix B. We first test the proposed algorithm on a 6-dof UR5 robotic manipulator with dynamics

$$\ddot{x} = B(x)^{-1}\left(u - C(\bar{x})\dot{x} - g(x) + d(\bar{x}, t)\right) \tag{9}$$

where $x, \dot{x} \in \mathbb{R}^6$ are the vectors of robot joint angles and angular velocities, respectively; $B(x) \in \mathbb{R}^{6\times6}$ is the positive definite inertia matrix, $C(\bar{x}) \in \mathbb{R}^{6\times6}$ is the Coriolis matrix, $g(x) \in \mathbb{R}^6$ is the gravity vector, and $d(\bar{x}, t) \in \mathbb{R}^6$ is a vector of friction terms and exogenous time-varying disturbances.

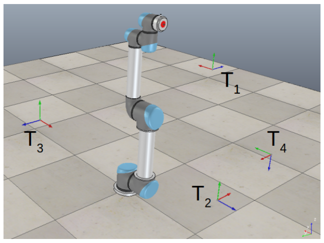

Figure 2: A UR5 robot in a workspace with four points of interest T_i, $i \in \{1, \ldots, 4\}$.

The workspace consists of four points of interest T_1, T_2, T_3, T_4 (end-effector position and Euler-angle orientation), as depicted in Fig. 2, which correspond to the joint-angle vectors c_1, c_2, c_3, c_4. More information is provided in Appendix A. We consider a nominal

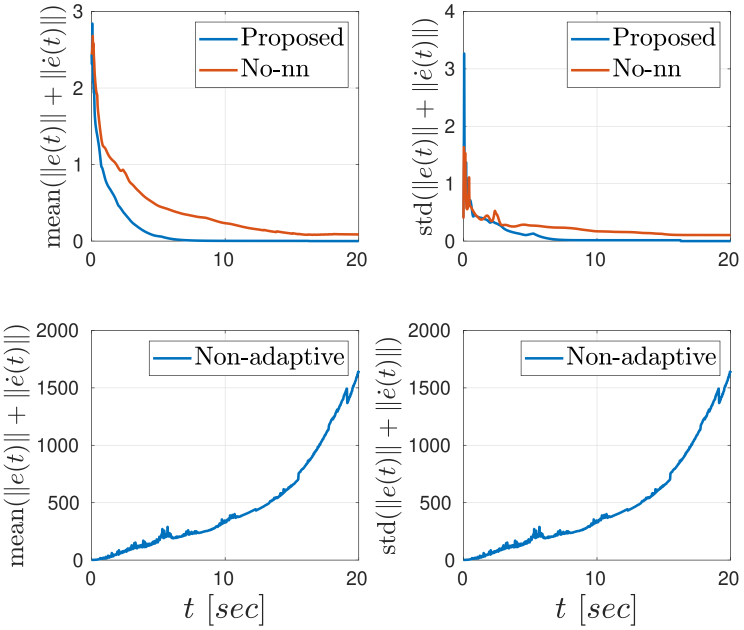

Figure 3: Mean (left) and standard deviation (right) of $\|e(t)\| + \|\dot{e}(t)\|$ for the proposed, non-adaptive, and no-neural-network control policies.

SITL task of the form $\phi = \bigwedge_{i \in \{1,\dots,4\}} G_{[0,\infty)} F_{I_i}(\|x_1 - c_i\| \leq 0.1)$, i.e., visit of x_1 to $c_i \in \mathbb{R}^6$ (within the radius 0.1) infinitely often within the time intervals dictated by I_i, for $i \in \{1,\dots,4\}$.

We create 150 problem instances by varying the positions of c_i, the time intervals I_i, the dynamic parameters of the robot (masses and moments of inertia of the robot's links and actuators), the friction and disturbance term $d(\cdot)$, the initial position and velocity of the robot, and the sequence of visits to the points c_i, as dictated by ϕ, i.e., one instance might correspond to the visit sequence $((x(0),0) \rightarrow (c_1, t_{1_1}) \rightarrow (c_2, t_{1_2}) \rightarrow (c_3, t_{1_3}) \rightarrow (c_4, t_{1_4})$, and another to $((x(0),0) \rightarrow (c_3, t_{1_3}) \rightarrow (c_1, t_{1_1}) \rightarrow (c_4, t_{1_4}) \rightarrow (c_2, t_{1_2})$. We separate the aforementioned 150 problem instances into 100 training instances and 50 test instances. We generate trajectories using the 100 training instances from system runs that satisfy different variations of one cycle of ϕ (i.e., one visit to each point). Each trajectory consists of 500 points and is generated using a nominal model-based controller. We use these trajectories to train a neural network and we test the control policy (4) in the 50 test instances. We also compare our algorithm with the non-adaptive controller $u_c(\bar{x}, t) = u_{\text{nn}}(x, t) - k_1 e - k_2 \dot{e}$, as well as with a modified version $u_d(\bar{x}, t)$ of (4) that does not employ the neural network (i.e., the term $u_{\text{nn}}(\bar{x}, t)$). The comparison results are depicted in Fig. 3, which depicts the mean and standard deviation of the signal $\|e(t)\| + \|\dot{e}(t)\|$ for the 50 instances and 20 seconds. It is clear from the figure that the proposed algorithm performs better than the non-adaptive and no-neural-network policies both in terms of convergence speed and steady-state error. It is worth noting that the non-adaptive policy results on average in unstable closed-loop system.

We next test the proposed algorithm, following a similar procedure, on a unicycle robot with dynamics of the form (5). Fig. 5 depicts the mean and standard deviation of the errors $e_d(t)$, $e_\beta(t)$ for 50 test instances. We note that the performance of the no-neural-network control policy is much more similar to the proposed one than in the UR5 case. This can be attributed to (1) the lack of gravitational terms in the unicycle dynamics, which often lead to instability, and (2) the chosen control gains of the no-neural-network policy, which are sufficiently large to counteract the effect of the dynamic uncertainties.

Finally, we compare the performance of the proposed control policy with the reported data of (Wang et al. (2019)) on the benchmarking enivronment of the *pendulum*, where a single-link mechanical structure aims to reach the upright position[4]. Following (Wang

[4] For the sake of comparison, we do not consider an SITL task here.

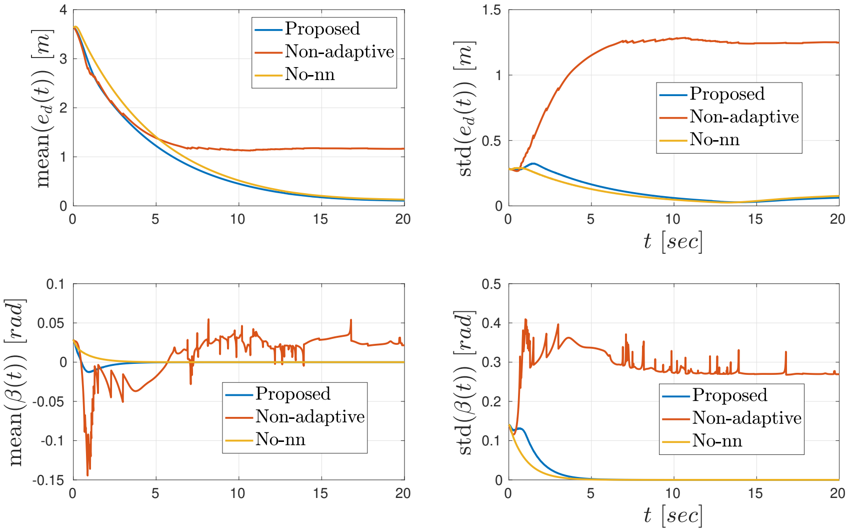

Figure 5: Mean (left) and standard deviation (right) of $e_d(t)$, $\beta(t)$ for the proposed, non-adaptive, and no-neural-network control policies.

et al. (2019)), the reward and costs are $r_{pend}(t) = -\cos q(t) - 0.1 \sin q(t) - 0.1\dot{q}(t) - 0.001u(t)^2$ and $J_{pend} = \sum_{t=1}^{H} \gamma^t r_{pend}(t)$, respectively. Similar to the previous cases and in contrast to Wang et al. (2019), we generate 150 instances by varying the system parameters (pendulum length and mass), the external disturbances, and the initial conditions. We generate 100 trajectories, consisting of 500 points each, for the 100 training instances, by employing a nominal controller, and we use them train a neural network. Moreover, in order to guarantee the feasibility of the proposed algorithm (4) we consider larger control-action bounds than in (Wang et al. (2019)). The original bounds render these systems under-actuated, which is not included in the considered class of systems (1) and consist part of our future work. It should be noted that such larger bounds affect negatively the acquired rewards. We test the control policy (4) on the 50 test instances, for 5000 steps each, corresponding to 10 seconds. We set $H = 200$ and $\gamma = 1$ (Wang et al. (2019)). Fig. 4 depicts the mean and standard deviation of the time-varying reward and cost functions, illustrating successful regulation to the upright position. After 5000 steps, we obtain a mean reward and cost of 0.99 and 200, respectively, showing better performance than the reported cost of 180 in (Wang et al. (2019)). Moreover, the proposed control algorithm achieves this performance without resorting to exhaustive exploration of the state-space, which is the case in the reinforcement-learning algorithms used in (Wang et al. (2019)). This is a very important property in practical engineering systems, where safety is of paramount significance and certain areas of the state space must be avoided.

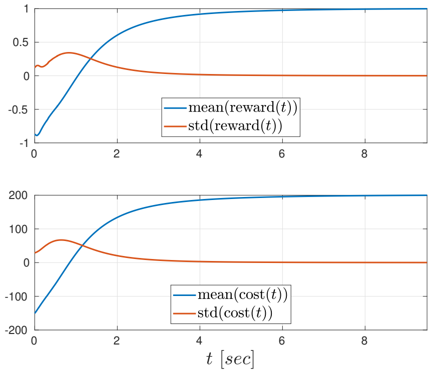

Figure 4: Mean and standard deviation of the reward and cost for the pendulum environment.

5 Discussion and Limitations

As shown in the experimental results, the control algorithm is able to accomplish tasks which were not considered when generating the training data. Similarly, the trajectories used in the training data were generated using systems with different dynamical parameters, and not specifically the ones used in the tests. The aforementioned attributes signify the ability of the proposed algorithm to generalize to different tasks and systems with different parameters. Nevertheless, it should be noted that the control algorithm (5) guarantees asymptotic stability properties, without characterizing the system's transient state. Hence, task specifications that require fast system response (e.g., a robot needs to travel a long distance in a short time horizon) would possibly necessitate large control gains in order to achieve fast convergence to the derived open-loop trajectory. The derivation of transient-state bounds and their relation with the given task specification (as for instance in (Verginis & Dimarogonas (2018))) is left for future work. Moreover, the proposed control policy is currently limited by systems satisfying Assumption 1 and is not able to take into account under-actuated systems (e.g., the acrobot or cart-pole system); such systems consist part of our future work. Finally, the discontinuities of (4), (8) might be problematic and create chattering when implemented in real actuators. A continuous approximation that has shown to yield satisfying performance is the boundary-layer technique (Slotine et al. (1991)).

6 Conclusion and Future Work

We develop a novel control algorithm for the control of robotic systems with unknown nonlinear dynamics subject to task specifications expressed as SITL constraints. The algorithm integrates neural network-based learning and adaptive control. We provide formal guarantees and perform extensive numerical experiments. Future directions will focus on relaxing the considered assumptions and extending the proposed methodology to underactuated systems.

7 Reproducibility statement

We provide the proofs of the theoretical results, i.e., Theorem 1 and Corollary 1, in Appendix A. Additionally, we elaborate on the required assumptions (Assumptions 1, 2, 3) throughout the text - see pages 3, 5, and 7. Finally, we provide implementation details, instructions, and the respective code, required to reproduce the results, in Appendix B and the supplementary material.

References

Charalampos P Bechlioulis and George A Rovithakis. A low-complexity global approximation-free control scheme with prescribed performance for unknown pure feedback systems. *Automatica*, 50 (4):1217–1226, 2014.

Thomas Berger, Huy Hoàng Lê, and Timo Reis. Funnel control for nonlinear systems with known strict relative degree. *Automatica*, 87:345–357, 2018.

Felix Berkenkamp and Angela P Schoellig. Safe and robust learning control with gaussian processes. *European Control Conference (ECC)*, pp. 2496–2501, 2015.

Dimitri Bertsekas. Lessons from alphazero for optimal, model predictive, and adaptive control. *arXiv preprint arXiv:2108.10315*, 2021.

Dimitri Bertsekas and John Tsitsiklis. *Neuro-Dynamic Programming*. Athena Scientific, MIT, 1996.

Mingyu Cai, Mohammadhosein Hasanbeig, Shaoping Xiao, Alessandro Abate, and Zhen Kan. Modular deep reinforcement learning for continuous motion planning with temporal logic. *arXiv preprint arXiv:2102.12855*, 2021.

Alberto Camacho and Sheila A McIlraith. Towards neural-guided program synthesis for linear temporal logic specifications. *arXiv preprint arXiv:1912.13430*, 2019.

M Capotondi, G Turrisi, C Gaz, Valerio Modugno, Giuseppe Oriolo, and A De Luca. An online learning procedure for feedback linearization control without torque measurements. *Conference on Robot Learning*, pp. 1359–1368, 2020.

Zhiyong Chen. Nussbaum functions in adaptive control with time-varying unknown control coefficients. *Automatica*, 102:72–79, 2019.

Tao Cheng, Frank L Lewis, and Murad Abu-Khalaf. A neural network solution for fixed-final time optimal control of nonlinear systems. *Automatica*, 43(3):482–490, 2007.

George Cybenko. Approximation by superpositions of a sigmoidal function. *Mathematics of control, signals and systems*, 2(4):303–314, 1989.

Kenji Doya. Efficient nonlinear control with actor-tutor architecture mozer, jordan, petsche (eds.) advances in neural information processing systems 9. 1997.

Bo Fan, Qinmin Yang, Xiaoyu Tang, and Youxian Sun. Robust adp design for continuous-time nonlinear systems with output constraints. *IEEE transactions on neural networks and learning systems*, 29(6):2127–2138, 2018.

Nicholas Fischer, Rushikesh Kamalapurkar, and Warren E Dixon. Lasalle-yoshizawa corollaries for nonsmooth systems. *IEEE Transactions on Automatic Control*, 58(9):2333–2338, 2013.

Christopher Hahn, Frederik Schmitt, Jens U Kreber, Markus N Rabe, and Bernd Finkbeiner. Teaching temporal logics to neural networks. *arXiv preprint arXiv:2003.04218*, 2020.

F Hong, SS Ge, B Ren, and TH Lee. Robust adaptive control for a class of uncertain strict-feedback nonlinear systems. *International Journal of Robust and Nonlinear Control: IFAC-Affiliated Journal*, 19(7):746–767, 2009.

Haimin Hu, Mahyar Fazlyab, Manfred Morari, and George J Pappas. Reach-sdp: Reachability analysis of closed-loop systems with neural network controllers via semidefinite programming. *IEEE Conference on Decision and Control (CDC)*, pp. 5929–5934, 2020.

Jiangshuai Huang, Wei Wang, Changyun Wen, and Jing Zhou. Adaptive control of a class of strict-feedback time-varying nonlinear systems with unknown control coefficients. *Automatica*, 93: 98–105, 2018a.

Xiucai Huang, Yongduan Song, and Junfeng Lai. Neuro-adaptive control with given performance specifications for strict feedback systems under full-state constraints. *IEEE transactions on neural networks and learning systems*, 30(1):25–34, 2018b.

Edouard Ivanjko, Toni Petrinic, and Ivan Petrovic. Modelling of mobile robot dynamics. *7th EUROSIM Congress on Modelling and Simulation*, 2, 2010.

Radoslav Ivanov, James Weimer, Rajeev Alur, George J Pappas, and Insup Lee. Verisig: verifying safety properties of hybrid systems with neural network controllers. *Proceedings of the 22nd ACM International Conference on Hybrid Systems: Computation and Control*, pp. 169–178, 2019.

Achin Jain, Truong Nghiem, Manfred Morari, and Rahul Mangharam. Learning and control using gaussian processes. *ACM/IEEE International Conference on Cyber-Physical Systems (ICCPS)*, pp. 140–149, 2018.

Girish Joshi, Jasvir Virdi, and Girish Chowdhary. Asynchronous deep model reference adaptive control. *Conference on Robot Learning*, 2020.

Rushikesh Kamalapurkar, Huyen Dinh, Shubhendu Bhasin, and Warren E Dixon. Approximate optimal trajectory tracking for continuous-time nonlinear systems. *Automatica*, 51:40–48, 2015.

Bahare Kiumarsi, Kyriakos G Vamvoudakis, Hamidreza Modares, and Frank L Lewis. Optimal and autonomous control using reinforcement learning: A survey. *IEEE transactions on neural networks and learning systems*, 29(6):2042–2062, 2017.

M. Krstic, I. Kanellakopoulos, and P. Kokotovic. Nonlinear and Adaptive Control Design. *Publisher: Wiley New York*, 1995.

Kevin Leahy, Eric Cristofalo, Cristian-Ioan Vasile, Austin Jones, Eduardo Montijano, Mac Schwager, and Calin Belta. Control in belief space with temporal logic specifications using vision-based localization. *The International Journal of Robotics Research*, 38(6):702–722, 2019.

Lars Lindemann and Dimos V Dimarogonas. Efficient automata-based planning and control under spatio-temporal logic specifications. *American Control Conference (ACC)*, pp. 4707–4714, 2020.

Lars Lindemann, Christos K Verginis, and Dimos V Dimarogonas. Prescribed performance control for signal temporal logic specifications. *IEEE Conference on Decision and Control (CDC)*, pp. 2997–3002, 2017.

Ke Liu, Robert Tokar, and Brain McVey. An integrated architecture of adaptive neural network control for dynamic systems. *Advances in neural information processing systems*, 7:1031–1038, 1994.

Wenliang Liu, Noushin Mehdipour, and Calin Belta. Recurrent neural network controllers for signal temporal logic specifications subject to safety constraints. *IEEE Control Systems Letters*, 2021.

Meiyi Ma, Ji Gao, Lu Feng, and John Stankovic. Stlnet: Signal temporal logic enforced multivariate recurrent neural networks. *Advances in Neural Information Processing Systems*, 33, 2020.

Emilio Tanowe Maddalena, CG da S Moraes, Gierri Waltrich, and Colin N Jones. A neural network architecture to learn explicit mpc controllers from data. *IFAC-PapersOnLine*, 53(2):11362–11367, 2020.

Lipo Mo, Xiaolin Yuan, and Yongguang Yu. Neuro-adaptive leaderless consensus of fractional-order multi-agent systems. *Neurocomputing*, 339:17–25, 2019.

Julian Nubert, Johannes Köhler, Vincent Berenz, Frank Allgöwer, and Sebastian Trimpe. Safe and fast tracking on a robot manipulator: Robust mpc and neural network control. *IEEE Robotics and Automation Letters*, 5(2):3050–3057, 2020.

Brad Paden and Shankar Sastry. A calculus for computing filippov's differential inclusion with application to the variable structure control of robot manipulators. *IEEE transactions on circuits and systems*, 34(1):73–82, 1987.

Ryan Riegel, Alexander Gray, Francois Luus, Naweed Khan, Ndivhuwo Makondo, Ismail Yunus Akhalwaya, Haifeng Qian, Ronald Fagin, Francisco Barahona, Udit Sharma, et al. Logical neural networks. *arXiv preprint arXiv:2006.13155*, 2020.

Ankit Jayesh Shah, Pritish Kamath, Shen Li, and Julie A Shah. Bayesian inference of temporal task specifications from demonstrations. 2018.

Bruno Siciliano, Lorenzo Sciavicco, Luigi Villani, and Giuseppe Oriolo. Modelling, planning and control. *Advanced Textbooks in Control and Signal Processing. Springer,*, 2009.

Jean-Jacques E Slotine, Weiping Li, et al. *Applied nonlinear control*, volume 199. Prentice hall Englewood Cliffs, NJ, 1991.

Chuangchuang Sun and Kyriakos G Vamvoudakis. Continuous-time safe learning with temporal logic constraints in adversarial environments. *American Control Conference (ACC)*, pp. 4786–4791, 2020.

Richard S Sutton and Andrew G Barto. *Reinforcement learning: An introduction*. MIT press, 2018.

Kyriakos G Vamvoudakis and Frank L Lewis. Online actor–critic algorithm to solve the continuous-time infinite horizon optimal control problem. *Automatica*, 46(5):878–888, 2010.

Christos Verginis and Dimos V Dimarogonas. Asymptotic tracking of second-order nonsmooth feedback stabilizable unknown systems with prescribed transient response. *IEEE Transactions on Automatic Control*, 2020.

Christos K Verginis and Dimos V Dimarogonas. Timed abstractions for distributed cooperative manipulation. *Autonomous Robots*, 42(4):781–799, 2018.

Christos K. Verginis, Dimos V. Dimarogonas, and Lydia E. Kavraki. Kdf: Kinodynamic motion planning via geometric sampling-based algorithms and funnel control. 2021.

Draguna Vrabie and Frank Lewis. Neural network approach to continuous-time direct adaptive optimal control for partially unknown nonlinear systems. *Neural Networks*, 22(3):237–246, 2009.

Chuanzheng Wang, Yinan Li, Stephen L Smith, and Jun Liu. Continuous motion planning with temporal logic specifications using deep neural networks. *arXiv preprint arXiv:2004.02610*, 2020.

Tingwu Wang, Xuchan Bao, Ignasi Clavera, Jerrick Hoang, Yeming Wen, Eric Langlois, Shunshi Zhang, Guodong Zhang, Pieter Abbeel, and Jimmy Ba. Benchmarking model-based reinforcement learning. *arXiv preprint arXiv:1907.02057*, 2019.

Ruixuan Yan and Agung Julius. Neural network for weighted signal temporal logic. *arXiv preprint arXiv:2104.05435*, 2021.

Yongliang Yang, Kyriakos G Vamvoudakis, and Hamidreza Modares. Safe reinforcement learning for dynamical games. *International Journal of Robust and Nonlinear Control*, 30(9):3706–3726, 2020.

Ssu-Hsin Yu, Anuradha M Annaswamy, DS Touretzky, MC Mozer, and ME Hasselmo. Neural control for nonlinear dynamic systems. *Advances in Neural Information Processing Systems*, pp. 1010–1016, 1996.

Jingang Zhao and Minggang Gan. Finite-horizon optimal control for continuous-time uncertain nonlinear systems using reinforcement learning. *International Journal of Systems Science*, 51(13): 2429–2440, 2020.

Yaofeng Desmond Zhong and Naomi Leonard. Unsupervised learning of lagrangian dynamics from images for prediction and control. *Advances in Neural Information Processing Systems*, 33, 2020.

A Appendix

We provide here the proof of Theorem 1 and Corollary 1. We first give some preliminary notation and background on systems with discontinuous dynamics.

Notation

Given a function $f : \mathbb{R}^n \to \mathbb{R}^k$, its Filippov regularization is defined as (Paden & Sastry (1987))

$$\mathsf{K}[f](x) := \bigcap_{\delta>0} \bigcap_{\mu(\bar{N})=0} \overline{\text{co}}(f(\mathcal{B}(x,\delta)\backslash\bar{N}),t), \tag{10}$$

where $\bigcap_{\mu(\bar{N})=0}$ is the intersection over all sets $\bar{N}$ of Lebesgue measure zero, $\overline{\text{co}}(E)$ is the closure of the convex hull $\text{co}(E)$ of the set E, and $\mathcal{B}(x,\delta)$ is the ball with radius δ centered at x.

Nonsmooth Analysis

Consider the following differential equation with a discontinuous right-hand side:

$$\dot{x} = f(x,t), \tag{11}$$

where $f : \mathcal{D} \times [t_0, \infty) \to \mathbb{R}^n$, $\mathcal{D} \subset \mathbb{R}^n$, is Lebesgue measurable and locally essentially bounded.

Definition 1 (Def. 1 of (Fischer et al. (2013)))**.** *A function $x : [t_0, t_1) \to \mathbb{R}^n$, with $t_1 > t_0$, is called a Filippov solution of (11) on $[t_0, t_1)$ if $x(t)$ is absolutely continuous and if, for almost all $t \in [t_0, t_1)$, it satisfies $\dot{x} \in \mathsf{K}[f](x,t)$, where $\mathsf{K}[f](x,t)$ is the Filippov regularization of $f(x,t)$.*

Lemma 1 (Lemma 1 of (Fischer et al. (2013)))**.** *Let $x(t)$ be a Filippov solution of (11) and $V : \mathcal{D} \times [t_0, t_1) \to \mathbb{R}$ be a locally Lipschitz, regular function[5]. Then $V(x(t),t)$ is absolutely continuous, $\dot{V}(x(t),t) = \frac{\partial}{\partial t}V(x(t),t)$ exists almost everywhere (a.e.), i.e., for almost all $t \in [t_0, t_1)$, and $\dot{V}(x(t),t) \overset{a.e}{\in} \dot{\tilde{V}}(x(t),t)$, where*

$$\dot{\tilde{V}} := \bigcap_{\xi \in \partial V(x,t)} \xi^\top \begin{bmatrix} \mathsf{K}[f](x,t) \\ 1 \end{bmatrix},$$

and $\partial V(x,t)$ is Clarke's generalized gradient at (x,t) (Fischer et al. (2013)).

[5] See (Fischer et al. (2013)) for a definition of regular functions.

Corollary 2 (Corollary 2 of (Fischer et al. (2013)))**.** *For the system given in (11), let $\mathcal{D} \subset \mathbb{R}^n$ be an open and connected set containing $x = 0$ and suppose that f is Lebesgue measurable and $x \mapsto f(x,t)$ is essentially locally bounded, uniformly in t. Let $V : \mathcal{D} \times [t_0, t_1) \to \mathbb{R}$ be locally Lipschitz and regular such that $W_1(x) \leq V(x,t) \leq W_2(x)$, $\forall t \in [t_0, t_1)$, $x \in \mathcal{D}$, and*

$$z \leq -W(x(t)), \;\; \forall z \in \dot{\tilde{V}}(x(t), t), \; t \in [t_0, t_1), \; x \in \mathcal{D},$$

where W_1 and W_2 are continuous positive definite functions and W is a continuous positive semi-definite on $\mathcal{D}$. Choose $r > 0$ and $c > 0$ such that $\bar{\mathcal{B}}(0,r) \subset \mathcal{D}$ and $c < \min_{\|x\|=r} W_1(x)$. Then for all Filippov solutions $x : [t_0, t_1) \to \mathbb{R}^n$ of (11), with $x(t_0) \in \mathbb{D} := \{x \in \bar{\mathcal{B}}(0,r) : W_2(x) \leq c\}$, it holds that $t_1 = \infty$, $x(t) \in \mathbb{D}$, $\forall t \in [t_0, \infty)$, and $\lim_{t\to\infty} W(x(t)) = 0$.

Proof of Theorem 1. We re-write first the condition of Assumption 2. Note that $p_{\mathrm{d}}(t)$ and its derivatives are bounded functions of time. Moreover, since $e = x - p_{\mathrm{d}}$, $\dot{e} = \dot{x} - \dot{p}_{\mathrm{d}}$, it holds that $\|\bar{x}\| \leq \|e\| + \|\dot{e}\| + \|p_{\mathrm{d}}\| + \|\dot{p}_{\mathrm{d}}\|$ and $\dot{v}_{\mathrm{d}} = \ddot{p}_{\mathrm{d}} - k_1 \dot{e}$, as well as $e_v = \dot{x} - v_{\mathrm{d}} = \dot{e} + k_1 e$ implying $\dot{e} = e_v - k_1 e$. Therefore, in view of (2), one can find positive constants d_1, d_2, D such that

$$\frac{1}{\underline{g}} \|\underline{g} e + f(\bar{x},t) + g(\bar{x},t) u_{\mathrm{nn}}(\bar{x},t) - \dot{v}_{\mathrm{d}}\| \leq d_1 \|e\| + d_2 \|e_v\| + D, \tag{12}$$

for all $\bar{x} \in \mathbb{R}^{2n}$, $t \geq 0$, where $\underline{g}$ is the minimum eigenvalue of $g(\bar{x},t)$, which is positive owing to the positive definitiveness of $g(\cdot)$. Inequality (12) will be used later in the proof.

Let now a constant α such that $\frac{d_1 \alpha}{2} < k_1$. As will be clarified later, the adaptation variables $\hat{\ell}_1$, $\hat{\ell}_2$ aim to approximate the constants $\frac{d_1}{2\alpha} + d_2$ and D, respectively. Therefore, let $\ell_1 := \frac{d_1}{2\alpha} + d_2$, $\ell_2 := D$, and the respective error terms $\widetilde{\ell}_1 := \hat{\ell}_1 - \ell_1$, $\widetilde{\ell}_2 := \hat{\ell}_2 - \ell_2$, as well as the overall state $\widetilde{x} := [e^\top, e_v^\top, \widetilde{\ell}_1, \widetilde{\ell}_2]^\top \in \mathbb{R}^{2n+2}$. Since the control policy is discontinuous, we use the notion of Filippov solutions. The Filippov regularization of u is $\mathsf{K}[u] = u_{\mathrm{nn}}(x,t) - k_2 e_v - \hat{\ell}_1 e_v - \hat{\ell}_2 \hat{\mathsf{E}}_v$, where $\hat{\mathsf{E}}_v := \frac{e_v}{\|e_v\|}$ if $e_v \neq 0$ and $\hat{\mathsf{E}}_v \in (-1,1)$ otherwise. Note that, in any case, it holds that $e_v^\top \hat{\mathsf{E}}_v = \|e_v\|$.

Let now the continuously differentiable function

$$V(\widetilde{x}) := \frac{1}{2}\|e\|^2 + \frac{1}{2\underline{g}}\|e_v\|^2 + \sum_{i\in\{1,2\}} \frac{1}{2k_{\ell_i}} \widetilde{\ell}_i$$

which satisfies $W_1(\widetilde{x}) \leq V(\widetilde{x}) \leq W_2(\widetilde{x})$ for $W_1(\widetilde{x}) := \min\{\frac{1}{2}, \frac{1}{2\underline{g}}, \frac{1}{2k_{\ell_1}}, \frac{1}{2k_{\ell_2}}\}\|\widetilde{x}\|^2$, $W_2(\widetilde{x}) := \max\{\frac{1}{2}, \frac{1}{2\underline{g}}, \frac{1}{2k_{\ell_1}}, \frac{1}{2k_{\ell_2}}\}\|\widetilde{x}\|^2$. According to Lemma 1, $\dot{V}(\widetilde{x}) \overset{a.e.}{\in} \dot{\tilde{V}}(\widetilde{x})$, with $\dot{\tilde{V}} := \bigcap_{\xi \in \partial V(\widetilde{x})} \mathsf{K}[\dot{\widetilde{x}}]$. Since $V(\widetilde{x})$ is continuously differentiable, its generalized gradient reduces to the standard gradient and thus it holds that $\dot{\tilde{V}}(\widetilde{x}) = \nabla V^\top \mathsf{K}[\dot{\widetilde{x}}]$, where $\nabla V = [e^\top, \frac{1}{\underline{g}} e_v^\top, \frac{1}{k_{\ell_1}}\widetilde{\ell}_1, \frac{1}{k_{\ell_2}}\widetilde{\ell}_2]^\top$. By differentiating V and using (3), one obtains

$$\dot{V} \subset \widetilde{W}_s := e^\top(\dot{x} - \dot{p}_{\mathrm{d}}) + \frac{1}{\underline{g}} e_v^\top \big(f(\bar{x},t) + g(\bar{x},t)u - \dot{v}_{\mathrm{d}}\big) + \frac{1}{k_{\ell_1}} \widetilde{\ell}_1 \dot{\hat{\ell}}_1 + \frac{1}{k_{\ell_2}} \widetilde{\ell}_2 \dot{\hat{\ell}}_2$$

and by using $\dot{x} = e_v + v_{\mathrm{d}}$ and substituting the control policy (3), (4), and inequality (12),

$$\begin{aligned}
\widetilde{W}_s :=& - k_1\|e\|^2 + \frac{1}{\underline{g}} e_v^\top \big(\underline{g} e + f(\bar{x},t) + g(\bar{x},t) u_{\mathrm{nn}}(\bar{x},t) - \dot{v}_{\mathrm{d}}\big) - \frac{1}{\underline{g}} e_v^\top g(\bar{x},t)\big(k_2 e_v + \hat{\ell}_1 e_v + \hat{\ell}_2 \hat{\mathsf{E}}_v\big) \\
&+ \widetilde{\ell}_1 \|e_v\|^2 + \widetilde{\ell}_2 \|e_v\| \\
\leq& - k_1\|e\|^2 + d_1\|e_v\|\|e\| + d_2\|e_v\|^2 + D\|e_v\| - \frac{1}{\underline{g}} e_v^\top g(\bar{x},t)\big(k_2 e_v + \hat{\ell}_1 e_v + \hat{\ell}_2 \hat{\mathsf{E}}_v\big) \\
&+ \widetilde{\ell}_1 \|e_v\|^2 + \widetilde{\ell}_2 \|e_v\|
\end{aligned}$$

Note from (4) and the fact that $\hat{\ell}_1(0) > 0$, $\hat{\ell}_2(0) > 0$ that $\hat{\ell}_1(t) > 0$ and $\hat{\ell}_2(t)) > 0$ for all $t \geq 0$. Moreover, recall that $g(\bar{x},t)$ is positive definite for all $\bar{x} \in \mathbb{R}^{2n}$, $t \geq 0$, with $\underline{g}$ being its minimum (and positive) eigenvalue. Therefore, we conclude that $\widetilde{W}_s$ becomes

$$\widetilde{W}_s \leq - k_1\|e\|^2 + d_1\|e_v\|\|e\| + d_2\|e_v\|^2 + D\|e_v\| - (k_2 + \hat{\ell}_1)\|e_v\|^2 - \hat{\ell}_2\|e_v\| + \widetilde{\ell}_1\|e_v\|^2 + \widetilde{\ell}_2\|e_v\|$$

By incorporating the term α in the term $d_1\|e_v\|\|e\|$, we obtain $d_1\|e_v\|\|e\| = d_1\alpha\frac{\|e_v\|}{\alpha}\|e\|$ and by using the property $ab \leq \frac{1}{2}a^2 + \frac{1}{2}b^2$ for any constants a,b, we obtain $d_1\alpha\frac{\|e_v|}{\alpha}\|e\| \leq \frac{d_1\alpha}{2}\|e\|^2 + \frac{d_1}{2\alpha}\|e_v\|^2$. Therefore, $\widetilde{W}_s$ becomes

$$\begin{aligned}\widetilde{W}_s \leq &- \left(k_1 - \frac{d_1\alpha}{2}\right)\|e\|^2 + \left(\frac{d_1}{2\alpha} + d_2\right)\|e_v\|^2 + D\|e_v\| - (k_2 + \hat{\ell}_1)\|e_v\|^2 - \hat{\ell}_2\|e_v\| + \widetilde{\ell}_1\|e_v\|^2 + \widetilde{\ell}_2\|e_v\| \\ = &- \left(k_1 - \frac{d_1\alpha}{2}\right)\|e\|^2 + \ell_1\|e_v\|^2 + \ell_2\|e_v\| - (k_2 + \hat{\ell}_1)\|e_v\|^2 - \hat{\ell}_2\|e_v\| + \widetilde{\ell}_1\|e_v\|^2 + \widetilde{\ell}_2\|e_v\| \\ = &- \left(k_1 - \frac{d_1\alpha}{2}\right)\|e\|^2 - k_2\|e_v\|^2 =: -Q(\widetilde{x})\end{aligned}$$

Therefore, it holds that $\zeta \leq -Q(\widetilde{x})$, for all $\zeta \in \dot{\widetilde{V}}$, with Q being a continuous and positive semi-definite function in $\mathbb{R}^{2n+2}$, since $k_1 - \frac{d_1\alpha}{2} > 0$. Choose now any finite $r > 0$ and let $c < \min_{\|\widetilde{x}\|=r} W_1(\widetilde{x})$. Hence, all the conditions of Corollary 2 are satisfied and hence, all Filippov solutions starting from $\widetilde{x}(0) \in \Omega_f := \{\widetilde{x} \in \mathcal{B}(0, r) : \widetilde{W}_2(\widetilde{x}) \leq c\}$ are bounded and remain in Ω_f, satisfying $\lim_{t\to\infty} Q(\widetilde{x}(t)) = 0$. Note that r, and hence c, can be arbitrarily large allowing and finite initial condition $\widetilde{x}(0)$. Moreover, the boundedness of $\widetilde{x}$ implies the boundedness of e, $\dot{e}$, e_v, $\widetilde{\ell}_1$, and $\widetilde{\ell}_2$, and hence of $\hat{\ell}_1(t)$ and $\hat{\ell}_2(t)$, for all $t \in \mathbb{R}_{\geq 0}$. In view of (5), we finally conclude the boundendess of $u(\cdot)$, $\dot{\hat{\ell}}_1$, and $\dot{\hat{\ell}}_2$, for all $t \in \mathbb{R}_{\geq 0}$, leading to the conclusion of the proof.

□

Proof of Corollary 1. The derivatives of e_d, β in (6) can be written as

$$\begin{bmatrix}\dot{e}_d \\ \dot{\beta}\end{bmatrix} = G\begin{bmatrix}v \\ \omega\end{bmatrix} + \begin{bmatrix}\dot{p}_{\text{d},1}\cos(\phi+\beta) + \dot{p}_{\text{d},2}\sin(\phi+\beta) \\ \frac{\dot{p}_{\text{d},2}}{e_d}\cos(\phi+\beta) - \frac{\dot{p}_{\text{d},1}}{e_d}\sin(\phi+\beta)\end{bmatrix}$$

where

$$G := \begin{bmatrix}-\cos\beta & 0 \\ \frac{\sin\beta}{e_d} & -1\end{bmatrix}$$

It can be verified that the reference velocity signals, designed in (7), can be written as

$$\begin{bmatrix}v_\text{d} \\ \omega_\text{d}\end{bmatrix} = G^{-1}\begin{bmatrix}-\dot{p}_{\text{d},1}\cos(\phi+\beta) - \dot{p}_{\text{d},2}\sin(\phi+\beta) - k_d e_d \\ -\frac{\dot{p}_{\text{d},2}}{e_d}\cos(\phi+\beta) + \frac{\dot{p}_{\text{d},1}}{e_d}\sin(\phi+\beta) - k_\beta\beta\end{bmatrix}$$

and therefore, by using the relations $v = e_v + v_\text{d}$ and $\omega = e_\omega + \omega_\text{d}$, $\dot{e}_d$ and $\dot{\beta}$ can be written as

$$\begin{bmatrix}\dot{e}_d \\ \dot{\beta}\end{bmatrix} = \begin{bmatrix}-k_d e_d \\ -k_\beta\beta\end{bmatrix} + G\begin{bmatrix}e_v \\ e_\omega\end{bmatrix} = \begin{bmatrix}-k_d e_d \\ -k_\beta\beta\end{bmatrix} + \begin{bmatrix}-e_v\cos\beta \\ e_v\frac{\sin\beta}{e_d} - e_\omega\end{bmatrix} \tag{13}$$

The control design follows the back-stepping methodology (Krstic et al. (1995)). Let, therefore, the function $V_1 := \frac{1}{2}(e_d^2 + \beta^2)$, which, after time differentiation and use of (13), yields

$$\dot{V}_1 = -k_d e_d^2 - k_\beta\beta^2 - e_d e_v\cos\beta + \beta e_v\frac{\sin\beta}{e_d} - \beta e_\omega \tag{14}$$

We will cancel the two last terms of $\dot{V}_1$ using the control input (8).

First, we note that the inertia matrix of the system M, appearing in the unicycle dynamics (5), has the form (Ivanjko et al. (2010)) $M = \begin{bmatrix}M_1 & M_2 \\ M_2 & M_1\end{bmatrix}$ with $M_1 := \frac{mr^2}{4} + \frac{(I_C + md^2)r^2}{4R^2} + I_0$, $M_2 := \frac{mr^2}{4} - \frac{(I_C + md^2)r^2}{4R^2}$, and where I_C is the moment of inertia of the vehicle with respect to point C (see Fig. 1b), I_0 is the moment of inertia of the the wheels, and d is the distance of the between point C and the vehicle's center of mass (p_1, p_2). Therefore, the second part of the unicycle dynamics (5) can be written as

$$\begin{aligned}M_1\ddot{\theta}_R + M_2\ddot{\theta}_L &= u_R + f_{\theta,R}(\bar{x}, t) \\ M_2\ddot{\theta}_R + M_1\ddot{\theta}_L &= u_L + f_{\theta,L}(\bar{x}, t)\end{aligned}$$

with $f_{\theta,R}$ and $f_{\theta,L}$ denoting the elements of f_θ. By summing and subtracting the aforementioned equations, we obtain

$$(M_1 + M_2)(\ddot{\theta}_R + \ddot{\theta}_L) = u_R + u_L + f_{\theta,R}(\bar{x}, t) + f_{\theta,L}(\bar{x}, t) \tag{15a}$$

$$(M_1 - M_2)(\ddot{\theta}_R - \ddot{\theta}_L) = u_R - u_L + f_{\theta,R}(\bar{x}, t) - f_{\theta,L}(\bar{x}, t) \tag{15b}$$

From the definition of e_v and e_ω, it holds that $\dot{e}_v = \dot{v} - \dot{v}_{\mathrm{d}}$, $\dot{e}_\omega = \dot{\omega} - \dot{\omega}_{\mathrm{d}}$, which, by using the relations $v = \frac{r}{2}(\dot{\theta}_R + \dot{\theta}_L)$, $\omega = \frac{r}{2R}(\dot{\theta}_R - \dot{\theta}_L)$ and (15), becomes

$$\dot{e}_v = \frac{r}{2(M_1 + M_2)}\Big(u_R + u_L + f_{\theta,R}(\bar{x}, t) + f_{\theta,L}(\bar{x}, t)\Big) - \dot{v}_{\mathrm{d}} \tag{16a}$$

$$\dot{e}_\omega = \frac{r}{2R(M_1 - M_2)}\Big(u_R - u_L + f_{\theta,R}(\bar{x}, t) - f_{\theta,L}(\bar{x}, t)\Big) - \dot{\omega}_{\mathrm{d}} \tag{16b}$$

Define now $\ell_v := 2\frac{M_1+M_2}{r}$, $\ell_\omega := 2R\frac{M_1-M_2}{r}$. The adaptation terms $\hat{\ell}_v$, and $\hat{\ell}_\omega$, used in the control mechanism (8), aim to approximate ℓ_v and ℓ_ω, respectively. Note that $\hat{\ell}_v$ and $\hat{\ell}_\omega$ are positive, and we define the errors $\widetilde{\ell}_v := \hat{\ell}_v - \ell_v$, $\widetilde{\ell}_\omega := \hat{\ell}_\omega - \ell_\omega$.

We re-write next the condition of Assumption 3. It holds that $\|p\| = \sqrt{p_1^2 + p_2^2} \leq 2e_d + |p_{\mathrm{d},1}| + |p_{\mathrm{d},2}|$. Moreover, in view of (7) as well as the fact that $\beta \in (-\bar{\beta}, \bar{\beta}) \subset (-\frac{\pi}{2}, \frac{\pi}{2})$, where $\bar{\beta}$ is the bound of β, stated in Theorem 1, it holds that $|v| \leq |e_v| + |v_{\mathrm{d}}| \leq |e_v| + \frac{1}{\cos(\bar{\beta})}(|\dot{p}_{\mathrm{d},1}| + |\dot{p}_{\mathrm{d},2}| + k_d e_d)$, $|\omega| \leq |e_\omega| + |\omega_{\mathrm{d}}| \leq |e_\omega| + \frac{1}{\cos\bar{\beta}}(\alpha_1 + k_d) + k_\beta|\beta|$, where we also use the fact that $\frac{|\dot{p}_{\mathrm{d},1}\sin\phi - \dot{p}_{\mathrm{d},2}\cos\phi|}{e_d} \leq \alpha_1$. By also recalling that ϕ moves on the unit circle, we conclude that Assumption 3 becomes

$$\|f_\theta(\bar{x}, t) + u_{\mathrm{nn}}(\bar{x}, t)\| \leq d_d e_d + d_\beta|\beta| + d|e_v| + d|e_\omega| + D, \tag{17}$$

with $d_d := d(2 + \frac{k_d}{\cos\bar{\beta}})$, $d_\beta := dk_\beta$, and $D := d(2\bar{p}_{\mathrm{d}} + 2\pi + \frac{1}{\cos\bar{\beta}}(\alpha_1 + 2\bar{v}_{\mathrm{d}} + 1)$, where $\bar{p}_{\mathrm{d}}$ and $\bar{v}_{\mathrm{d}}$ are the upper bounds of $p_{\mathrm{d},i}$, $v_{\mathrm{d},i}$, respectively, $i \in \{1, 2\}$.

Let now positive constants γ_d and γ_β such that $k_d > 2d_d\gamma_d$ and $k_\beta > 2d_\beta\gamma_\beta$, and define

$$\ell_1 := \frac{d_d}{\gamma_d} + \frac{d_\beta}{\gamma_\beta} + 4d \tag{18}$$

which is the constant to be approximated by $\hat{\ell}_1$; its derivation will be clarified later. Let also $\ell_2 := 2D$, which we aim to approximate with the adaptation variable $\hat{\ell}_2$. We define hence the respective errors $\widetilde{\ell}_1 := \hat{\ell}_1 - \ell_1$ and $\widetilde{\ell}_2 := \hat{\ell}_2 - \ell_2$ and define the overall vector $\widetilde{x} := [e_d, \beta, e_v, e_\omega, \widetilde{\ell}_v, \widetilde{\ell}_\omega, \widetilde{\ell}_1, \widetilde{\ell}_2]^\top \in \mathbb{R}^8$. Since the control mechanism is discontinuous, we use again the notion of Filippov solutions. The Filippov regularization $\mathsf{K}[u]$ of u differs from u only in the terms $\hat{e}_v$ and $\hat{e}_\omega$, which are replaced by $\hat{\mathsf{E}}_v$, defined as $\hat{\mathsf{E}}_v := \frac{e_v}{|e_v|}$ if $e_v \neq 0$, and $\hat{\mathsf{E}}_v \in (-1, 1)$ otherwise, and $\hat{\mathsf{E}}_\omega$, defined as $\hat{\mathsf{E}}_\omega := \frac{e_\omega}{|e_\omega|}$ if $e_\omega \neq 0$, and $\hat{\mathsf{E}}_\omega \in (-1, 1)$, respectively.

Consider now the continuously differentiable and positive definite function

$$V(\bar{x}) := V_1 + \frac{\ell_v}{2}e_v^2 + \frac{\ell_\omega}{2}e_\omega^2 + \frac{1}{2k_v}\widetilde{\ell}_v^2 + \frac{1}{2k_\omega}\widetilde{\ell}_{\omega_i}^2 + \sum_{i\in\{1,2\}}\frac{1}{2k_i}\widetilde{\ell}_i^2$$

which satisfies $W_1(\widetilde{x}) \leq V(\widetilde{x}) \leq W_2(\widetilde{x})$ for $W_1(\widetilde{x}) := \min\{\frac{1}{2}, \frac{\ell_v}{2}, \frac{\ell_\omega}{2}, \frac{1}{2k_v}, \frac{1}{2k_\omega}, \frac{1}{2k_1}, \frac{1}{2k_2}\}\|\widetilde{x}\|^2$, $W_2(\widetilde{x}) := \max\{\frac{1}{2}, \frac{\ell_v}{2}, \frac{\ell_\omega}{2}, \frac{1}{2k_v}, \frac{1}{2k_\omega}, \frac{1}{2k_1}, \frac{1}{2k_2}\}\|\widetilde{x}\|^2$. According to Lemma 1, $\dot{V}(\widetilde{x}) \overset{a.e.}{\in} \dot{\widetilde{V}}(\widetilde{x})$, with $\dot{\widetilde{V}} := \bigcap_{\xi\in\partial V(\widetilde{x})}\mathsf{K}[\dot{\widetilde{x}}]$. Since $V(\widetilde{x})$ is continuously differentiable, its generalized gradient reduces to the standard gradient and thus it holds that $\dot{\widetilde{V}}(\widetilde{x}) = \nabla V^\top \mathsf{K}[\widetilde{x}]$, where $\nabla V = [e_d, \beta, \ell_v e_v, \ell_\omega e_\omega, \frac{1}{k_v}\widetilde{\ell}_v, \frac{1}{k_\omega}\widetilde{\ell}_\omega, \frac{1}{k_1}\widetilde{\ell}_1, \frac{1}{k_2}\widetilde{\ell}_2]^\top$. Therefore, by differentiating V and employing (14) and (15), we obtain

$$\begin{aligned}\dot{V} \subset \widetilde{W} :=& -k_d e_d^2 - k_\beta\beta^2 - e_d e_v\cos\beta + \beta e_v\frac{\sin\beta}{e_d} - \beta e_\omega + e_v\big(u_R + u_L + f_{\theta,R} + f_{\theta,L} - \ell_v\dot{v}_{\mathrm{d}}\big)\\ &+ e_\omega\big(u_R - u_L + f_{\theta,R} - f_{\theta,L} - \ell_\omega\dot{\omega}_{\mathrm{d}}\big) + \frac{1}{k_v}\widetilde{\ell}_v\dot{\hat{\ell}}_v + \frac{1}{k_\omega}\widetilde{\ell}_\omega\dot{\hat{\ell}}_\omega + \sum_{i\in\{1,2\}}\frac{1}{k_i}\widetilde{\ell}_i\dot{\hat{\ell}}_i\end{aligned}$$

By substituting the control and adaptation policy (8), $\widetilde{W}$ becomes

$$\begin{aligned}\widetilde{W} =& -k_d e_d^2 - k_\beta \beta^2 - k_v e_v^2 - k_\beta e_\omega^2 + e_v \dot{v}_{\mathrm{d}} \widetilde{\ell}_v + e_\omega \dot{\omega}_{\mathrm{d}} \widetilde{\ell}_\omega - \hat{\ell}_1(e_v^2 + e_\omega^2) - \hat{\ell}_2(|e_v| + |e_\omega|) \\ &+ e_v(u_{\mathrm{nn},R} + u_{\mathrm{nn},L} + f_{\theta,R} + f_{\theta,L}) + e_\omega(u_{\mathrm{nn},R} - u_{\mathrm{nn},L} + f_{\theta,R} - f_{\theta,L}) \\ &- \widetilde{\ell}_v e_v \dot{v}_{\mathrm{d}} - \widetilde{\ell}_\omega e_\omega \dot{\omega}_{\mathrm{d}} + \widetilde{\ell}_1(e_v^2 + e_\omega^2) + \widetilde{\ell}_2(|e_v| + |e_\omega|)\end{aligned}$$

where $u_{R,\mathrm{nn}}$ and $u_{L,\mathrm{nn}}$ are the elements of u_{nn}, i.e., $u_{\mathrm{nn}} = [u_{R,\mathrm{nn}}, u_{L,\mathrm{nn}}]^\top$. It is easy to conclude that $|u_{\mathrm{nn},R} + u_{\mathrm{nn},L} + f_{\theta,R} + f_{\theta,L}| \leq |u_{\mathrm{nn},R} + f_{\theta,R}| + |u_{\mathrm{nn},L} + f_{\theta,L}| \leq 2\|u_{\mathrm{nn}} + f_\theta\|$ and $|u_{\mathrm{nn},R} - u_{\mathrm{nn},L} + f_{\theta,R} - f_{\theta,L}| \leq |u_{\mathrm{nn},R} + f_{\theta,R}| + |u_{\mathrm{nn},L} + f_{\theta,L}| \leq 2\|u_{\mathrm{nn}} + f_\theta\|$ and hence, in view of (17),

$$\left.\begin{matrix} |u_{\mathrm{nn},R} + u_{\mathrm{nn},L} + f_{\theta,R} + f_{\theta,L}| \\ |u_{\mathrm{nn},R} - u_{\mathrm{nn},L} + f_{\theta,R} - f_{\theta,L}| \end{matrix}\right\} \leq \bar{D} := 2d_d e_d + 2d_\beta|\beta| + 2d|e_v| + 2d|e_\omega| + 2D$$

Therefore, $\widetilde{W}$ becomes

$$\begin{aligned}\widetilde{W} =& -k_d e_d^2 - k_\beta \beta^2 - k_v e_v^2 - k_\beta e_\omega^2 - \hat{\ell}_1(e_v^2 + e_\omega^2) - \hat{\ell}_2(|e_v| + |e_\omega|) + \bar{D}(|e_v| + |e_\omega|) \\ &+ \widetilde{\ell}_1(e_v^2 + e_\omega^2) + \widetilde{\ell}_2(|e_v| + |e_\omega|)\end{aligned}$$

The term $\bar{D}(|e_v| + |e_\omega|)$ yields

$$\begin{aligned}\bar{D}(|e_v| + |e_\omega|) =& 2d_d e_d|e_v| + 2d_\beta|\beta||e_v| + 2de_v^2 + 4d|e_v||e_\omega| + 2D|e_v| + 2d_d e_d|e_\omega| \\ &+ 2d_\beta|\beta||e_\omega| + 2de_\omega^2 + 2D|e_\omega|\end{aligned}$$

By setting $2d_d e_d|e_v| = 2d_d\gamma_d e_d \frac{|e_v|}{\gamma_d}$, $2d_d e_d|e_\omega| = 2d_d\gamma_d e_d \frac{|e_\omega|}{\gamma_d}$, and $2d_\beta|\beta||e_v| = 2d_\beta\gamma_\beta|\beta|\frac{|e_v|}{\gamma_\beta}$, $2d_\beta|\beta||e_\omega| = 2d_\beta\gamma_\beta|\beta|\frac{|e_\omega|}{\gamma_\beta}$ and completing the squares, one obtains

$$\begin{aligned}\bar{D}(|e_v| + |e_\omega|) \leq& 2d_d\gamma_d e_d^2 + 2d_\beta\gamma_\beta\beta^2 + \left(\frac{d_d}{\gamma_d} + \frac{d_\beta}{\gamma_\beta} + 4d\right)(e_v^2 + e_\omega^2) + 2D(|e_v| + |e_\omega|) \\ =& 2d_d\gamma_d e_d^2 + 2d_\beta\gamma_\beta\beta^2 + \ell_1(e_v^2 + e_\omega^2) + \ell_2(|e_v| + |e_\omega|)\end{aligned}$$

Hence, $\widetilde{W}$ becomes

$$\begin{aligned}\widetilde{W} \leq& -(k_d - 2d_d\gamma_d)e_d^2 - (k_\beta - 2d_\beta\gamma_\beta)\beta^2 - k_v e_v^2 - k_\beta e_\omega^2 - \hat{\ell}_1(e_v^2 + e_\omega^2) - \hat{\ell}_2(|e_v| + |e_\omega|) \\ &+ \ell_1(e_v^2 + e_\omega^2) + \ell_2(|e_v| + |e_\omega|) + \widetilde{\ell}_1(e_v^2 + e_\omega^2) + \widetilde{\ell}_2(|e_v| + |e_\omega|) \\ =& -(k_d - 2d_d\gamma_d)e_d^2 - (k_\beta - 2d_\beta\gamma_\beta)\beta^2 - k_v e_v^2 - k_\beta e_\omega^2 =: Q(\widetilde{x})\end{aligned}$$

Therefore, it holds that $\zeta \leq -Q(\widetilde{x})$, for all $\zeta \in \dot{\widetilde{V}}$, with Q being a continuous and positive semi-definite function in $\mathbb{R}^8$, since $k_d - 2d_d\gamma_d > 0$, $k_\beta - 2d_\beta\gamma_\beta > 0$. Choose now any finite $r > 0$ and let $c < \min_{\|\widetilde{x}\|=r} W_1(\widetilde{x})$. Hence, all the conditions of Corollary 2 are satisfied and hence, all Filippov solutions starting from $\widetilde{x}(0) \in \Omega_f := \{\widetilde{x} \in \mathcal{B}(0, r) : \widetilde{W}_2(\widetilde{x}) \leq c\}$ are bounded and remain in Ω_f, satisfying $\lim_{t\to\infty} Q(\widetilde{x}(t)) = 0$.

Note that r, and hence c, can be arbitrarily large allowing and finite initial condition $\widetilde{x}(0)$. Moreover, the boundedness of $\widetilde{x}$ implies the boundedness of e, $\dot{e}$, e_v, $\widetilde{\ell}_1$, and $\widetilde{\ell}_2$, and hence of $\hat{\ell}_1(t)$ and $\hat{\ell}_2(t)$, for all $t \in \mathbb{R}_{\geq 0}$. Finally, in view of the conditions $\frac{|\sin\phi\dot{p}_{\mathrm{d},1} - \cos\phi\dot{p}_{\mathrm{d},2}|}{e_d} < \alpha_1$ and $\frac{\sin\beta}{e_d} < \alpha_2$, one concludes the boundedness of all closed-loop signals, for all $t \geq 0$

□

B Appendix

We provide here more information on the experimental results of Section 4. All the results were obtained on MATLAB environment using the ODE simulator. We performed the training of the neural networks in with the pytorch library in Python environment. The neural networks consist of 4 fully connected layers of 512 neurons; each layer is followed by a batch normalization module and a ReLU activation function. For the training we use the adam optimizer and the mean-square-error loss function. In all cases we choose a batch size of 256, and we train until a desirable average (per batch) loss of the order of 10^{-4} is achieved. All the values of the data used for the training were normalized in $[0,1]$.

Regarding the robotic-arm task, the points of interest are set as $T_1 = [-0.15, -0.475, 0.675, \frac{\pi}{2}, 0, 0]^\top$, $T_2 = [-0.6, 0, 2.5, 0, -\frac{\pi}{2}, -\frac{\pi}{2}]^\top$, $T_3 = [-0.025, 0.595, 0.6, -\frac{\pi}{2}, 0, \pi]^\top$, and $T_4 = [-0.525, -0.55, 0.28, \pi, 0, -\frac{\pi}{2}]^\top$, and the corresponding joint-angle vectors as $c_1 = [-0.07, -1.05, 0.45, 2.3, 1.37, -1.33]^\top$, $c_2 = [1.28, 0.35, 1.75, 0.03, 0.1, -1.22]^\top$, $c_3 = [-0.08, 0.85, -0.23, 2.58, 2.09, -2.36]^\top$, $c_4 = [-0.7, -0.76, -1.05, -0.05, -3.08, 2.37]^\top$ (radians).

We set a nominal value for the time intervals as $I_i = [0, 20]$ (seconds), and we create 150 problem instances by varying the following attributes: firstly, we add uniformly random offsets in $[-0.3, 0.3]$ (radians) to the elements of all c_i, and in $[-2, 2]$ (seconds) to the right end-points of the intervals I_i; secondly, we add random offsets to the dynamic parameters of the robot (masses and moments of inertia of the robot's links and actuators) and we set a different friction and disturbance term $d(\cdot)$, leading to a different dynamic model in (9); thirdly, we set different sequences of visits to the points c_i, $i \in \{1, \dots, 4\}$, as dictated by ϕ, i.e., one trajectory might correspond to the visit sequence $((x(0), 0) \to (c_1, t_{1_1}) \to (c_2, t_{1_2}) \to (c_3, t_{1_3}) \to (c_4, t_{1_4})$, and another to $((x(0), 0) \to (c_3, t_{1_3}) \to (c_1, t_{1_1}) \to (c_4, t_{1_4}) \to (c_2, t_{1_2})$. Finally, we add uniformly random offsets in $[-0.5, 0.5]$ to the initial position of the robot (from the first point of the sequence), and we set its initial velocity randomly in the interval $[0, 1]^6$.

Regarding the dynamics (9), we use the methodology described in (Siciliano et al. (2009)) to derive the B, C, and g terms. We set nominal link masses and moments of inertia as $m = [1, 2.5, 5.7, 3.9, 2.5, 2.5, 0.7]$ (kg) and $I = [0.02, 0.04, 0.06, 0.05, 0.04, 0.04, 0.01]$ (kgm^2), respectively, and we add random offsets in $(-\frac{m}{2}, \frac{m}{2})$, $(-\frac{I}{2}, \frac{I}{2})$ in the created instances. Regarding the function $d()$ used in (9); we set $d(\bar{x}, t) = d_t(t) + d_f(\bar{x})$, where

$$d_t = A_t \begin{bmatrix} \sin(\eta_1 t + \varphi_1) \\ \vdots \\ \sin(\eta_6 t + \varphi_6) \end{bmatrix}, \quad d_f = R_t A_t \dot{x}$$

$A_t = \mathrm{diag}\{\, A_{t_i} \}_{i \in \{1, \dots, 6\}} \in \mathbb{R}^{6 \times 6}$, A_{t_i} is a random term in $(0, 2m_i)$, η_i is a random term in $(0, 1)$, φ_i is a random term in $(0, 2)$, and $R_t \in \mathbb{R}^{6 \times 6}$ is a matrix whose rows are set as $R_{t_i} \dot{x}_i$ and where $R_{t_i} \in \mathbb{R}^{6 \times 6}$ is a diagonal matrix whose diagonal elements take random values in $\{0, 1\}$. We chose the control gains of the control policy (4) as $k_1 = 1, k_2 = 10$, and $k_{\ell_1} = k_{\ell_2} = 10$.

Further experimental results are depicted in Figs. 6-10; Fig. 6a depicts the mean and standard deviation of $\|e_v(t)\|$ of the proposed control policy and no-neural-network one for the 50 test instances, whereas Figs. 9a depicts the control input that results from the control policy (4) as well as the the neural-network output. Note that the control input converges to the neural-network output, i.e., $\lim_{t \to \infty}(u(t) - u_{\text{nn}}(t)) = 0$, which can be also verified by (4) and the fact that $\lim_{t \to \infty} e_v(t) = 0$. Fig. 10a depicts the mean and standard deviation of the adaptation signals $\hat{\ell}_1(t)$, $\hat{\ell}_2(t)$ for the 50 test instances. Finally, Fig. 8 shows timestamps of one of the test trajectories, illustrating the visit of the robot end-effector to the points of interest at the pre-specified time stamps.

Regarding the unicycle experiments, the dynamic terms in (5) have the form

$$M = \begin{bmatrix} M_1 & M_2 \\ M_2 & M_1 \end{bmatrix}$$
$$f_\theta(\bar{x}, t) = d(\bar{x}, t)$$

with $M_1 := \frac{mr^2}{4} + \frac{(I_C + md^2)r^2}{4R^2} + I_0$, $M_2 := \frac{mr^2}{4} - \frac{(I_C + md^2)r^2}{4R^2}$, and where I_C is the moment of inertia of the vehicle with respect to point C (see Fig. 1b), I_0 is the moment of inertia of the the wheels, and d is the distance of the between point C and the vehicle's center of mass (p_1, p_2). The term $d(\bar{x}, t)$ is chosen as in the robotic-manipulator case. The points to visit are chosen here as $c_1 = [0, 0]^\top$, $c_2 = [0, 2]^\top$, $c_3 = [2, 0]^\top$, $c_4 = [2, 2]^\top$ and I_i is chosen as $I_i = [0, 20]$, $i \in \{1, \dots, 4\}$. We derive 150 problem instances by varying the following attributes: we vary c_i with random offsets in $[-0.3, 0.3]$ and the right end-points of I_i with random offsets in $[-2, 2]$; we add random offsets

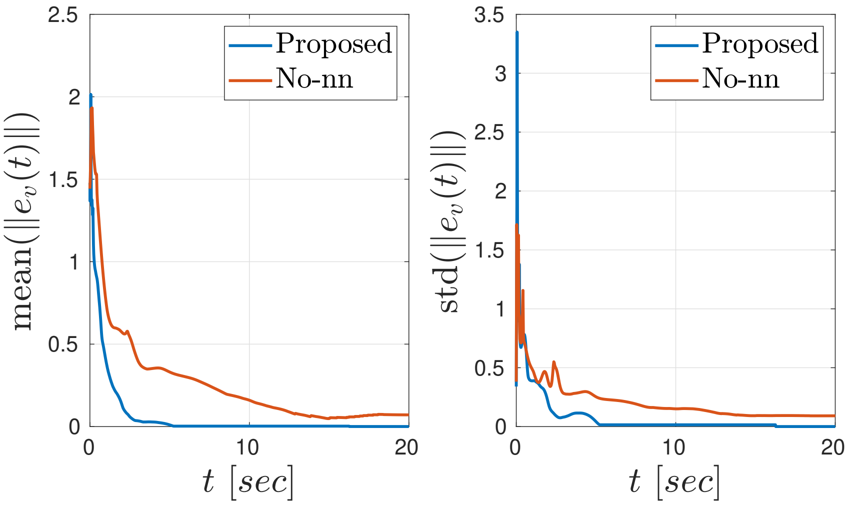

Figure 6: Mean (left) and standard deviation (right) of $e_v(t)$ for the proposed and no-neural-network control policies.

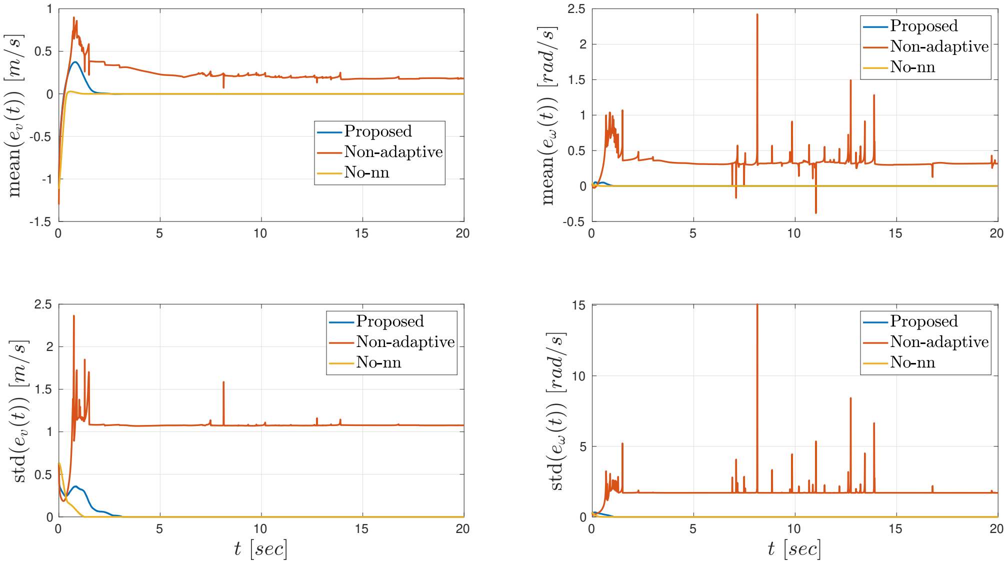

Figure 7: Mean (top) and standard deviation (bottom) of $e_v(t)$ and $e_\omega(t)$ for the proposed, non-adaptive, and no-neural-network control policies.

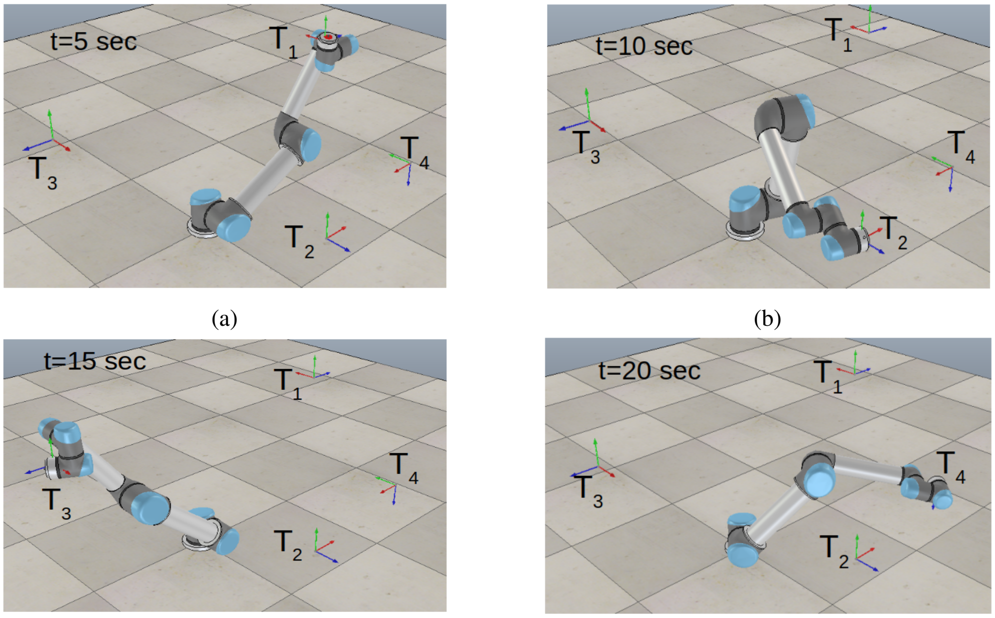

(a)

(b)

(c)

(d)

Figure 8: Illustration of the execution of one of the test trajectories of the UR5 robotic arm, visiting the points of interest at the pre-specified time stamps.

to the dynamic parameters (elaborated subsequently) and the function $d(\bar{x}, t)$, and we set different sequences of visits to the points c_i; we further vary the unicycle's initial position from the first c_i with random offsets in $[-0.3, 0.3]$, and its initial orientation with random offsets in $[-0.25, 0.25]$ (rad) from $\theta(0) = \arctan(e_2(0)/e_1(0))$; we further set random values in $[-0.25, 0.25]$ (rad/s) to the initial wheel velocities.

We set nominal values for the dynamic and geometric parameters, appearing in the inertia matrix, as $m = 28$ (kg), $I_C = 0.1$ (kgm^2), $I_0 = 0.01$ (kgm^2), $r = 0.01$ (m), $d = 0.01$ (m), and we added random offsets in $(-\frac{m}{2}, \frac{m}{2})$, $(-\frac{I_A}{2}, \frac{I_A}{2})$, $(-\frac{I_0}{2}, \frac{I_0}{2})$, $(-\frac{r}{2}, \frac{r}{2})$, $(-\frac{d}{2}, \frac{d}{2})$, respectively, for the problem instances. We chose the control gains of (8) as $k_d = 0.25$, $k_\beta = 1$, $k_v = k_\omega = k_{\ell_1} = k_{\ell_2} = 10$, $k_v = k_\omega = 1$. The non-adaptive control policy we compared our algorithm with was selected as

$$u_S = M_S \dot{v}_\text{d} - k_v e_v + e_d \cos\beta - \beta \frac{\sin\beta}{e_d}$$
$$u_D = M_D \dot{\omega}_\text{d} - k_\omega e_\omega + \beta$$

where v_d, ω_d are chosen as (7) and M_S, M_D are static estimates of $2\frac{M_1+M_2}{r}$, $2R\frac{M_1-M_2}{r}$, respectively. More specifically, we set a deviation of 25% in the parameters appearing in these terms to form M_S and M_D. Further experimental results are depicted in Figs. 6-10; Fig. 6b depicts the mean and standard deviation of the velocity errors $e_v(t)$, $e_\beta(t)$ for the 50 test instances, showing convergence to zero, whereas Figs. 9b depicts the control input that results from the control policy (4) as well as the the neural-network output. Similarly to the robotic-manipulator case, the control input converges to the neural-network output. Finally, Fig. 10b depicts the mean and standard deviation of the adaptation signals $\hat{\ell}_v(t)$, $\hat{\ell}_\beta(t)$, $\hat{\ell}_1(t)$, $\hat{\ell}_2(t)$ for the 50 test instances.

Finally, regarding the pendulum environment, we consider the dynamics

$$\ddot{q} = \frac{g}{L}\sin q + u + d(t)$$

where L is the pendulum's link length, g is the gravitational constant, and $d(t)$ is a term of exogenous disturbances. We created 150 instances by varying the mass and link length of the pendulum, the external disturbances, and setting its initial position and velocity randomly in $[-1, 1]$ (rad) and $[-1, 1]$ (rad/s), respectively. We selected unitary value for its nominal link length, and we added random

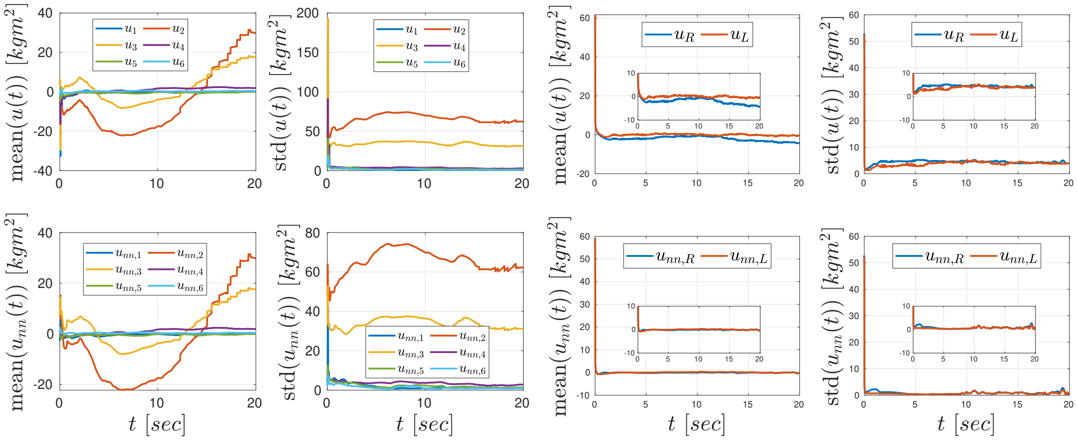

(a) (b)

Figure 9: (a): Mean (left) and standard deviation (right) of $u(t)$ (top) and $u_{\text{nn}}(t)$ (bottom) for the proposed control policy and the robotic-manipulator environment. (b): Mean and standard deviation (right) of $u(t)$ (top) and $u_{\text{nn}}(t)$ (bottom) for the proposed control policy and the unicycle environment.

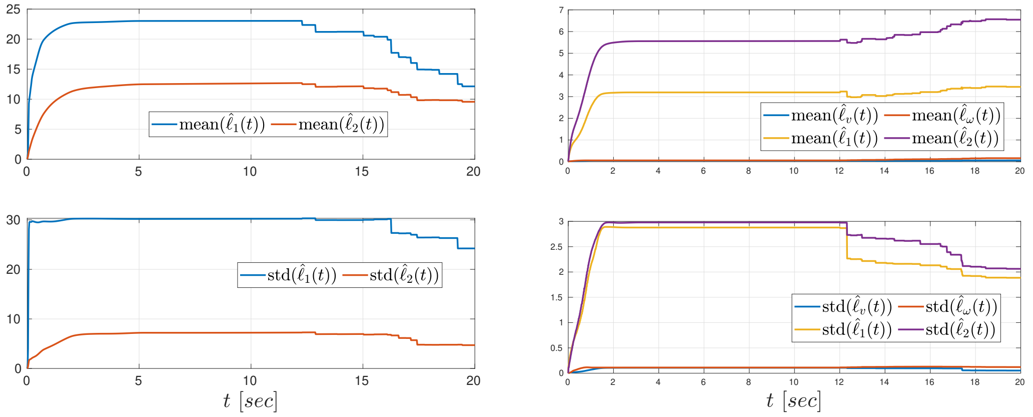

(a) (b)

Figure 10: (a): Mean (top) and standard deviation (bottom) of $\hat{\ell}_1(t)$, $\hat{\ell}_2(t)$ for the proposed control policy and the robotic-manipulator environment. (b): Mean (top) and standard deviation (bottom) of $\hat{\ell}_v(t)$, $\hat{\ell}_\omega(t)$, $\hat{\ell}_1(t)$, $\hat{\ell}_2(t)$ for the proposed control policy and the unicycle environment.

offsets in $(-0.5, 0.5)$ in each instance. We set the external disturbances as $d = A\sin(\eta t + \phi)$, with A, η, and ϕ taking random values in $[0, 0.2]$, $[0, 1]$, $[0, 2]$, respectively. In contrast to the robotic manipulator case, we assume feedback of $\sin q$, $\cos q$, $\dot{q}$, and set the error e in (3) as $1 - \cos(q - \pi)$. Finally, we chose the control gains as $k_1 = k_2 = 1$, and $k_{\ell_1} = k_{\ell_2} = 10$.